

SMC-NCA: Semantic-guided Multi-level Contrast for Semi-supervised Temporal Action Segmentation

Feixiang Zhou, Zheheng Jiang, Huiyu Zhou and Xuelong Li, *Fellow, IEEE*

Abstract—Semi-supervised temporal action segmentation (SS-TAS) aims to perform frame-wise classification in long untrimmed videos, where only a fraction of videos in the training set have labels. Recent studies have shown the potential of contrastive learning in unsupervised representation learning using unlabelled data. However, learning the representation of each frame by unsupervised contrastive learning for action segmentation remains an open and challenging problem. In this paper, we propose a novel Semantic-guided Multi-level Contrast scheme with a Neighbourhood-Consistency-Aware unit (SMC-NCA) to extract strong frame-wise representations for SS-TAS. Specifically, for representation learning, SMC is first used to explore intra- and inter-information variations in a unified and contrastive way, based on action-specific semantic information and temporal information highlighting relations between actions. Then, the NCA module, which is responsible for enforcing spatial consistency between neighbourhoods centered at different frames to alleviate over-segmentation issues, works alongside SMC for semi-supervised learning (SSL). Our SMC outperforms the other state-of-the-art methods on three benchmarks, offering improvements of up to 17.8% and 12.6% in terms of Edit distance and accuracy, respectively. Additionally, the NCA unit results in significantly better segmentation performance in the presence of only 5% labelled videos. We also demonstrate the generalizability and effectiveness of the proposed method on our Parkinson’s Disease Mouse Behaviour (PDMB) dataset. The code is publicly available at <https://github.com/FeixiangZhou/SMC-NCA>.

Index Terms—Action segmentation, Semi-supervised learning, Contrastive learning, Mouse social behaviour, Parkinson’s disease (PD).

I. INTRODUCTION

ACTION recognition on trimmed videos has achieved remarkable performance over the past few years [1]–[5]. Despite the success of these approaches on trimmed videos with a single action, their ability to handle long videos containing multiple actions with different lengths is limited. Temporal action segmentation (TAS) aims at temporally detecting and recognising human action segments in a long untrimmed video [6]–[8], which has attracted a lot of attention in recent years. Different from temporal action detection (TAD) [9] that detects the temporal boundaries (i.e., start and end) of action instances and predicts corresponding action categories simultaneously using temporally sparse action annotations, the goal of TAS is to produce frame-wise dense action labels. Besides, TAD

F. Zhou Z. Jiang and H. Zhou are with School of Computing and Mathematical Sciences, University of Leicester, United Kingdom. E-mail: {fz64; zj87; hz143}@leicester.ac.uk. H. Zhou is the corresponding author. The supplementary material is available at [Supp.](#), which includes additional experiments and explanations.

X. Li is with School of Artificial Intelligence, Optics and Electronics (iOPEN), Northwestern Polytechnical University, Xi’an 710072, P.R. China. E-mail: li@nwpu.edu.cn.

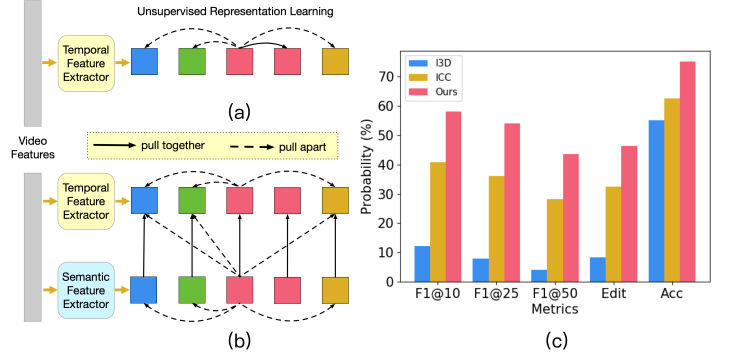


Fig. 1. Motivation of the proposed method. (a) ICC [25] only samples representations with temporal information for unsupervised contrastive representation learning, where the construction of both positive (red boxes with the same label) and negative (boxes with different colours) pairs is guided by input feature clustering. It is susceptible to clustering errors (see Fig. 2), leading to weaker frame-wise representations. (b) Our method leverages both temporal and semantic information to fully explore intra- and inter-information variations. We form positive pairs by considering the inherent temporal-semantic consistency of each frame, as well as three types of negative pairs based on the dynamic clustering of the original input, temporal and semantic features, thereby mitigating the adverse effects of clustering errors. (c) shows that our proposed method can learn more discriminative representations on the 50Salads dataset.

operates with general videos from everyday life, such as THUMOS14 [10], while TAS targets procedural activity datasets. It is a key task for analysing and understanding human activities in complex long videos, and has been widely applied in fields such as video surveillance [11], video summarization [12] and autonomous vehicles [13]. The temporal relations among sequential human actions are crucial in TAS as they determine the sequence and timing of each action. Recent research [14] reveals that semantic features based on label-text prompts can enhance action segmentation. Despite the impressive performance of the previous approaches [14]–[17], they rely on fully labelled videos where the start and end frames of each action are annotated, leading to substantial frame-wise annotation costs. To alleviate this problem, many researchers have started exploring weakly supervised approaches using transcripts [18]–[20], action sets [21]–[23] or annotated timestamps [24] to reduce the annotation cost whilst maintaining action segmentation performance. However, significant efforts are needed to produce partial labels for supervised learning. Recently, semi-supervised approaches [25]–[27] for this task have attracted increasing attention, with a small percentage of labelled videos in the training set.

SS-TAS is a non-trivial task as it often involves processing long untrimmed videos, presenting unique challenges com-

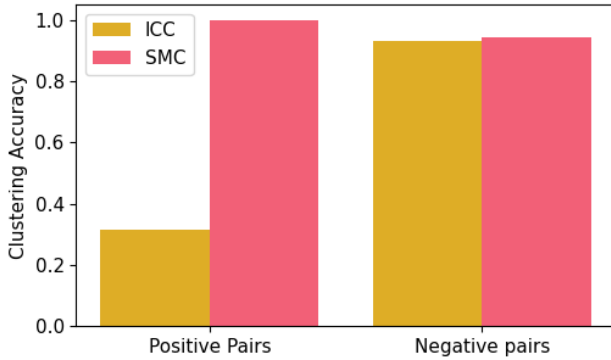


Fig. 2. Quantitative evidence that the quality of positive and negative pairs in ICC is affected by clustering errors. For both ICC and our SMC, we set the same batch size (5) and number of clusters (40), and the clustering accuracy is averaged over 50 epochs on the 50 Salads dataset by comparing the ground-truth labels with clustering labels. As observed, our SMC significantly improves the quality of positive pairs by leveraging the temporal-semantic consistency of each frame. The quality of negative pairs is also slightly enhanced by the dynamic clustering.

pared to trimmed sequences. It can be difficult to effectively utilising the complex information contained within these unlabelled videos while ensuring accurate segmentation. ICC [25] is the first attempt to explore semi-supervised learning for TAS by introducing a contrast-classify framework, which consists of two steps, i.e., unsupervised contrastive representation learning for frame-wise representation enhancement, as well as semi-supervised learning for action classification. As shown in Fig. 1(a), the contrastive learning approach in ICC primarily focuses on variations within temporal information containing relations between actions, which may ignore the potential role of action-specific semantic characteristics. Meanwhile, constructing both positive and negative sets for contrastive learning mainly depends on the clustering results (i.e., labels generated by clustering) of pre-trained input features. Empirical evidence has shown that the outcome of contrastive learning can be severely affected by clustering errors (see Fig. 2 and Tab. I (the first set of experiments)). Another method for this topic is leveraging the correlation of actions between the labelled and unlabelled videos, and temporal continuity of actions [26]. However, their method only relies on action frequency prior in labelled data to build such correlations, rendering it inadequate for guiding the learning of complex unlabelled videos. Consequently, how to effectively leverage unlabelled, long untrimmed videos is still an open and challenging problem.

In this paper, we propose SMC-NCA, a novel temporal-semantic contrast framework for SS-TAS. Our work is also built on the contrast-classify architecture, but unlike ICC, which contrasts relevant frames within temporal information alone, our SMC incorporates both temporal information (i.e., temporal relations between actions) and semantic information (i.e., action-specific characteristics) into a unified contrastive learning framework, effectively reducing clustering errors and promoting frame-wise representation learning. We further design a NCA unit to handle continuously fluctuating action category predictions, a.k.a. over-segmentation issues, leading

to better segmentation performance.

Inspired by the alignment of different augmented views of the same image/video [28]–[30], as well as that of multiple modalities [14], [31] (e.g., vision and language), we incorporate a simple semantic feature extractor to extract semantic information, which complements the temporal information for cross-information contrastive representation learning. Semantic information emphasises action-specific characteristics [14] in contrast to temporal information that encodes the dependencies between actions. Hence, we argue that leveraging the two types of information can help to facilitate representation learning (see Fig. 1(c)). As shown in Fig. 1(b), temporal and semantic branches are then jointly optimised by our SMC for fully exploring inter- and intra-information variations. Concretely, unlike [25] that recognises positive pairs based on the clustering results, SMC creates them (i.e., pairwise boxes connected by solid lines in Fig. 1(b)) by directly aligning temporal-semantic information, relying on the inherent temporal-semantic consistency of each frame. Meanwhile, we explicitly construct three types of complementary negative pairs to enlarge inter-class dissimilarity, where the generation process is determined by our proposed dynamic clustering algorithm. With the proposed temporal-semantic contrast, our SMC pays attention to action-specific semantic features and temporal relations simultaneously, effectively reducing the impact of clustering errors, thus achieving enhanced representations (see Tab. I).

Benefiting from strong representations learned by SMC, our approach offers a significant improvement on the semi-supervised frame-wise accuracy. However, there still exist significant over-segmentation errors [32] when we use a small amount of labelled data for training the system, resulting in low-quality segmentation results, i.e., segmental F1 score and Edit distance (see Tab. V). This is because the existing contrast-classify framework excessively emphasises frame-wise classification performance by carefully performing inter-frame contrast to enhance the discriminability of each frame’s representation, thus potentially overlooking the consistency of categories within a particular action segment. To this end, we propose NCA to encourage the consistency between neighbourhoods (i.e., action segments) centered at different frames. Intuitively, feature distributions within the neighbourhoods of frames with the same label should be spatially close. NCA can be combined with SMC to deal with over-segmentation issues, particularly when we conduct supervised learning with a small amount of labelled data.

Our main contributions are highlighted as follows:

- We propose SMC-NCA, a novel temporal-semantic contrast framework tailored for SS-TAS, where temporal information with relations between actions, and semantic information with action-specific attributes are jointly utilised to enhance representation learning.
- We propose SMC for unsupervised representation learning, allowing one to fully explore intra- and inter-information variations for learning discriminative frame-wise representations with the support of semantic information.

- We propose NCA to alleviate over-segmentation problems in semi-supervised settings by enforcing inter-neighbourhood consistency. This enables significant improvement in the segmentation quality while maintaining good frame-wise accuracy.
- Experimental results demonstrate that our SMC-NCA outperforms state-of-the-art methods across different settings of labelled data (5%, 10%, 40% and 100%) on three challenging datasets.
- We also introduce a new Parkinson’s Disease Mouse Behaviour (PDMB) dataset, which provides a valuable resource for the research community to investigate the behavioural correlations of mice with Parkinson’s Disease. Experimental results show that our method is generalizable and effective on different kinds of datasets beyond human actions.

II. RELATED WORK

A. Temporal Action Segmentation

Temporal action segmentation (TAS) has been an increasingly popular trend in the domain of video understanding, which involves different levels of supervision. Fully-supervised methods require that each frame in the training videos be labelled. Earlier approaches have attempted to incorporate high-level temporal modelling over frame-wise classifiers. Kuehne et al. [34] utilised Fisher vectors of improved dense trajectories to represent video frames, and modelled each action with a Hidden Markov Model (HMM). Singh et al. [35] used a two-stream network to learn representations of short video chunks, which are then fed into a bi-directional LSTM to capture dependencies between different chunks. However, their approaches are computationally intensive due to sequential prediction. Most recent approaches employ TCN (temporal convolutional network) [6], [15], [33], GCN (graph convolution network) [17], [36] or Transformer [16] to model the long-range temporal dependencies in the videos. In spite of their promising performance, obtaining annotations on fine-grained actions for each frame is costly. Weakly-supervised methods mainly focus on transcript-level (with action order information) [18]–[20], set-level (without action order information) [21]–[23] and timestamp-level [24] supervisions to reduce the annotation effort. However, necessary supervision information is also needed for each video in the training set. Unsupervised approaches [37]–[40] take advantage of clustering algorithms without any supervised signal per video, which still suffer from poor performance compared to other supervised settings.

B. Unsupervised Contrastive Representation Learning

Visual representation plays a crucial role in various computer vision tasks, including temporal action segmentation [16], [35], person retrieval [41], [42] and event detection [43]. It can be learned in different ways, including fully supervised, semi-supervised and unsupervised methods. For instance, Shi et al. [42] proposed to mine various human attributes and model relations between them to learn precise

attribute representations. Shen et al. [43] explored multi-modal information fusion to enrich video content representations.

Recently, contrastive representation learning has been extensively used in different computer vision applications such as image representation learning [28], [44]–[46], video representation learning [29], [30], [47]–[50], time series representation learning [51]–[53], face recognition [54]–[56]. Among these approaches, contrastive loss [28], [44] and triplet loss [53], [54] are two popular loss functions to perform contrasting. The underlying idea behind the former is to pull together representations of augmented samples of the same image or video clips (i.e., positive pair) while pulling apart those of different instances (i.e., negative pair). The latter has the same goal but involves defining a triplet of (*anchor*, *positive* and *negative pairs*), where the positive pairs (i.e., anchor and positive representations) should be close and the negative pairs (i.e., anchor and negative representations) should be far apart.

The idea of visual-semantic alignment for representation enhancement has been explored in various fields such as few-shot learning [57], [58], meta learning [59] and out-of-distribution detection [60]. Different from most methods that operate within a supervised setting where label information is utilised to guide feature/image alignment, our SMC performs temporal-semantic contrast in an unsupervised way to fully utilise unlabelled videos. Furthermore, it is based on the triplet loss [53], which effectively reduces the dependence on noisy clustering labels, and leverages complementary information between temporal and semantic information compared with other methods.

C. Semi-supervised Learning

Semi-supervised learning (SSL) is a good solution to reduce the cost of data labelling, which leverages a few labelled samples and a large number of unlabeled samples to train the model. The current semi-supervised methods are mainly divided into prediction-based and representation-based approaches [61]. Prediction-based approaches typically involve regularizing the classifier’s prediction of unlabelled data, where two common paradigms for this purpose are pseudo-labelling [62]–[64] and consistency regularization [65]–[67]. Pseudo-labelling based methods generate pseudo labels for unlabeled data through pre-trained models and use these pseudo labels to further optimise the model. Consistency based methods encourage the model to make similar predictions on images obtained by applying different data augmentation techniques to the same image. For example, FixMatch [65] uses the model to generate pseudo labels for weakly augmented unlabeled images and only samples with highly-confident pseudo-labels will be used for training. To adapt FixMatch to video-based action recognition, Wu et al. [68] designed a neighbor-guided consistent and contrastive learning framework to reuse lowly-confident samples and learn more discriminative feature representations. However, prediction-based approaches are less effective compared to representation-based approaches in large-scale scenarios [61].

Representation-based methods focus more on the representations encoded by deep learning networks. Recent studies

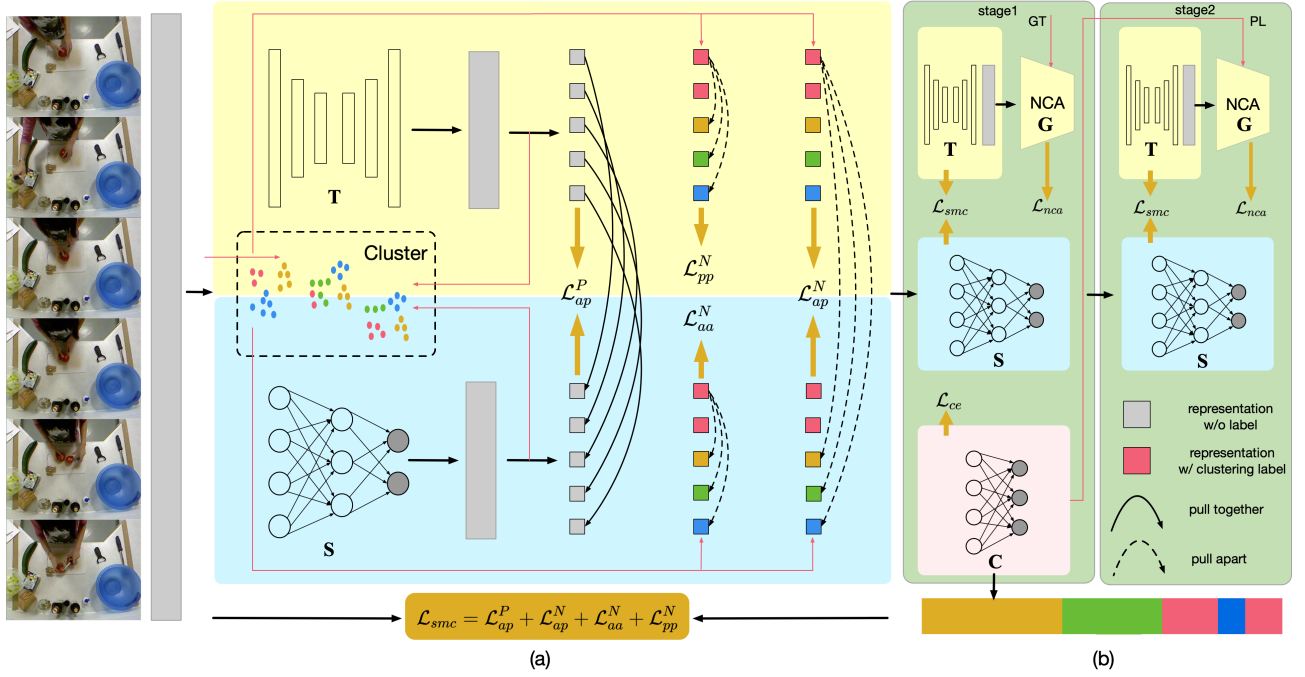


Fig. 3. Our proposed semi-supervised learning framework for temporal action segmentation. (a) Unsupervised representation learning. The pre-trained I3D features are fed into the long-term feature extractor T and the semantic feature extractor S to generate temporal and high-level semantic representations, respectively. Each kind of representation is sampled, followed by performing Semantic-guided Multi-level Contrast. (b) Semi-supervised learning. In stage 1, our Neighbourhood-Consistency-Aware unit G works closely with SMC, and the classification layer C can produce pseudo-labels (PL) used to guide the subsequent contrastive learning (stage 2). \mathcal{L}_{ap}^P , \mathcal{L}_{aa}^N and \mathcal{L}_{pp}^N denote the negative losses of three negative pairs which are driven by the clustering results. \mathcal{L}_{ap}^P represents the positive loss without relying on the clustering labels. \mathcal{L}_{nca} is generated in the NCA module. Note that T and C are two sub-networks of the C2F-TCN [25], [33] backbone. The former is responsible for temporal feature extraction, while the latter is connected after the former to perform action classification. S and G are only used for training in order to facilitate learning and will not be used during the inference stage.

exploit the success of self-supervised learning [28], [44] in learning representations from unlabeled data to train large-scale semi-supervised models [69], [70]. PAWS [71] proposed a single-stage training scheme that combines supervised and self-supervised learning for SSL. Although these methods have shown promise, it remains challenging to directly apply data augmentation strategies, such as flipping, rotation, and transformation, used in the image or video domain to TAS as the inputs are pre-computed feature vectors [26]. Inspired by [25], we propose a novel temporal-semantic contrast framework for representation enhancement, which shows strong frame-wise representations and segmentation performance.

III. PROPOSED METHOD

The overall framework of our SMC-NCA is illustrated in Fig. 3. For unsupervised representation learning, given the input video features, a temporal feature extractor T and semantic feature extractor S are jointly adopted to extract temporal and semantic information. Our SMC learns not only intra-information variation but also inter-information variation, where the temporal information describes the temporal dependencies between actions while semantic information highlights the action-specific characteristics. For semi-supervised learning, the models T , S and a linear classifier C are firstly integrated to perform supervised learning on a small number of labelled videos, followed by a new round of contrastive learning based on the pseudo-labels provided by

C . An additional NCA unit (G) is designed in conjunction with contrastive learning to measure the spatial consistency between different neighbourhoods for the alleviation of over-segmentation errors. Following [25], we iteratively perform classification and contrastive learning. We have not altered the structure of the backbone C2F-TCN [25]; instead, we introduce two additional modules, S and G , to facilitate unsupervised and semi-supervised learning. These two modules seamlessly integrate with the backbone and are exclusively utilised during model training to improve the semi-supervised segmentation performance. They are not utilised during the inference phase.

A. Preliminaries on Contrastive Learning

Contrastive loss. InfoNCE loss [28], [44], [45] is usually used for optimisation in unsupervised representation learning. It is calculated on images or video clips with the common goal of encouraging instances of the same class to be approaching, and pushing the instances of different classes apart from each other in the embedding space. Following the formalism of [25], [28], we define a set of features $\mathcal{F} = \{\mathbf{f}_i | i \in \mathcal{I}\}$, which is represented as a matrix \mathbf{F} ($\mathbf{F}[i] = \mathbf{f}_i$). \mathcal{I} denotes the set of feature indices and each feature \mathbf{f}_i has a unique class. Thus, given $\mathbf{F}[i]$, the positive set $\mathcal{P}_i \subset \mathcal{I}$ consisting of indices of features that have the same class as $\mathbf{F}[i]$, and the corresponding negative set \mathcal{N}_i , the contrastive loss for each $j \in \mathcal{P}_i$ is defined

as:

$$\mathcal{L}_{cont}(i, j) = -\log \frac{e^{\text{sim}(\mathbf{F}[i], \mathbf{F}[j])/\tau}}{e^{\text{sim}(\mathbf{F}[i], \mathbf{F}[j])/\tau} + \sum_{k \in \mathcal{N}_i} e^{\text{sim}(\mathbf{F}[i], \mathbf{F}[k])/\tau}} \quad (1)$$

where $\text{sim}(\mathbf{F}[i], \mathbf{F}[j]) = \mathbf{F}[i]^\top \mathbf{F}[j] / \|\mathbf{F}[i]\|_2 \|\mathbf{F}[j]\|_2$ is the inner product between two ℓ_2 normalised vectors. $\tau > 0$ is a temperature parameter.

Triplet loss. Unlike the contrastive loss, triplet loss [53], [54] requires to define a triplet $(\mathbf{F}[a], \mathbf{F}[p], \mathbf{F}[n])$ where $\mathbf{F}[a]$, $\mathbf{F}[p]$ and $\mathbf{F}[n]$ represent the anchor, positive and negative representations, respectively. This loss attracts positive pairs, $\mathbf{F}[a]$ (anchor) and $\mathbf{F}[p]$ (positive), while pushing away negative pairs, $\mathbf{F}[a]$ and $\mathbf{F}[n]$ (negative). Following [53], the triplet loss is formulated as:

$$\begin{aligned} \mathcal{L}_{trip}(a, p, n) = & -\log \left(\sigma(\mathbf{F}[a]^\top \mathbf{F}[p]) \right) \\ & -\log \left(\sigma(-\mathbf{F}[a]^\top \mathbf{F}[n]) \right) \end{aligned} \quad (2)$$

where σ is the sigmoid function. The core of the triplet loss is to effectively generate the three representations.

B. Problem Definition

A video sequence can be represented as $\mathbf{V} \in \mathbb{R}^{T \times E}$ where T is the total number of frames and E represents the dimension of the pre-trained I3D features [72]. Each video frame $\mathbf{V}[t] \in \mathbb{R}^E$ has a ground-truth action label $y[t] \in \{1, \dots, A\}$ where A denotes the number of the classes. We use an encoder-decoder model, i.e., C2F-TCN [33] as our base segmentation network \mathbf{T} . Therefore, given the input video features \mathbf{V} , we aim to learn the unsupervised model $(\mathbf{T} : \mathbf{S})$ by our Semantic-guided Multi-level Contrast on the dataset $\mathcal{D} = \mathcal{D}_U \cup \mathcal{D}_L$ (\mathcal{D}_U and \mathcal{D}_L denote the unlabelled and labelled videos, respectively) where \mathbf{T} and \mathbf{S} are the temporal and semantic models, respectively. Subsequently, the Neighbourhood-Consistency-Aware module \mathbf{G} and a linear mapping layer \mathbf{C} are added to form semi-supervised model $(\mathbf{T} : \mathbf{S} : \mathbf{G} : \mathbf{C})$ which is trained on a small subset of labelled training videos \mathcal{D}_L . We follow the standard operation of [25], where we first use the same down-sampling strategy to obtain coarser features (i.e., input) of temporal dimension T . In the inference, the final predictions are up-sampled to the original full resolution with temporal dimension T_{ori} to compare with the original ground truth.

C. Semantic-guided Multi-level Contrast

As mentioned earlier, we propose to leverage both temporal and semantic information to our proposed SMC scheme, where inter- and intra-information variations are jointly learned to enhance frame-wise representations.

Temporal and semantic information generation. To encode the correlation between actions, we adopt the C2F-TCN model to produce the multi-resolution representation and combine representations of different resolutions into a new representation using the same temporal up-sampling approach in [25]. Similar to [25], the combined representation with temporal information is used for unsupervised contrastive

learning, which is denoted as $\mathbf{X} = \mathbf{T}(\mathbf{V}) \in \mathbb{R}^{N \times T \times D}$, where N is the mini-batch size during training and D represents the feature dimension.

In ICC, only temporal information is utilised to perform inter-frame contrastive learning. In contrast, we propose to incorporate semantic information alongside temporal information for cross-information contrast. This decision is motivated by the significance of semantic features in capturing action-specific details, a factor that has been proven to be effective in promoting temporal action segmentation [14]. Different from extracting semantic features from action- or class-specific text information [14], we implicitly extract such features directly from the raw input features without the need for complex text encoding models. Specifically, we employ the multilayer perceptron (MLP) as a semantic feature extractor on the input video features \mathbf{V} to generate a new representation (denoted as $\mathbf{H} = \mathbf{S}(\mathbf{V}) \in \mathbb{R}^{N \times T \times D}$) with high-level semantic information. A MLP offers simplicity and efficiency (we also test other extractors, such as deeper MLPs and 1D CNNs, see Tab. III). The model \mathbf{S} can be formulated as:

$$\begin{aligned} \mathbf{V}^{(l+1)} &= \sigma \left(\mathbf{V}^{(l)} \mathbf{W}^{(l)} + b^{(l)} \right) \\ \mathbf{H} &= \mathbf{V}^{(l+1)} \mathbf{W}^{(l+1)} + b^{(l+1)} \end{aligned} \quad (3)$$

where $\mathbf{V}^{(l)} \in \mathbb{R}^{N \times T \times D^l}$ denotes the input hidden representation from the previous layer (with $\mathbf{V}^{(0)} = \mathbf{V}$) and $\mathbf{W}^{(l)} \in \mathbb{R}^{D^l \times D^{l+1}}$ and $b^{(l)}$ are trainable parameters. σ is an activation function. Temporal and semantic information complement each other in promoting representation learning as they capture different aspects of actions. Next, we will elaborate on how to incorporate these two types of information into a unified contrastive learning framework.

Inter-information variation learning. Under the guidance of clustering labels, ICC reduces the intra-class distance by bringing frames belonging to the same label closer together. However, it is susceptible to clustering errors. In practice, the distribution of data may be complex and uneven, leading the clustering algorithm to assign similar frames to different clusters or dissimilar frames to the same cluster. This clustering error can cause ICC to learn incorrect similarity information during training, thus affecting its performance. Additionally, clustering errors may result in overfitting to samples with noisy labels, thereby reducing its generalization ability.

With the support of semantic information, we directly construct inter-information positive pairs without relying on noisy clustering labels. To be more specific, we firstly sample a fixed number of frames from each training video to form a new temporal representation $\mathbf{X}_s \in \mathbb{R}^{N \times T_s \times D}$ and semantic representation $\mathbf{H}_s \in \mathbb{R}^{N \times T_s \times D}$ using the same sampling strategy reported in [25], where T_s is the number of the sampled frames from each video. This is because it is too computationally expensive to measure each frame of every video in a mini-batch. The sampled frames for each video are then combined by concatenation operation on the dimension T to form $\mathbf{X}_s \in \mathbb{R}^{N \cdot T_s \times D}$ and $\mathbf{H}_s \in \mathbb{R}^{N \cdot T_s \times D}$.

The features of pairwise video frames with the same index in \mathbf{X}_s and \mathbf{H}_s describe the same action (boxes connected by solid lines in Fig. 1(b)). In this way, we identify \mathbf{X}_s and \mathbf{H}_s as

positive and anchor representations respectively, and our goal is to pull them (i.e., positive pairs) together. Inspired by [53], given \mathbf{X}_s and \mathbf{H}_s , we formalise the objective function of the inter-information similarity learning as:

$$\begin{aligned} \Psi_{ap}^P &= - \left[\log \left(\sigma(\mathbf{H}_s^\top \mathbf{X}_s / \xi) \right) \right] \odot \mathbf{I} \\ &= \begin{bmatrix} \Psi_{ap}^P[1, 1] & & \\ & \ddots & \\ & & \Psi_{ap}^P[N \cdot T_s, N \cdot T_s] \end{bmatrix} \end{aligned} \quad (4)$$

where \odot represents the element-wise product. $\mathbf{I} \in \mathbb{R}^{N \cdot T_s \times N \cdot T_s}$ represents the identity matrix used to select pairwise frames with the same index, and $0 < \xi < 1$ is a scale factor to adjust the correlation between vectors. $\Psi_{ap}^P[., .]$ is the element of matrix Ψ_{ap}^P .

The advantages of optimising this function are twofold. Firstly, we consider the temporal and semantic information simultaneously, which is beneficial to improving the ability of representation learning. Secondly, learning of positive pairs (anchor and positive representations) is not dependent on the coarse clustering results, compared to ICC which generates related contrastive instances based on clustering results. In contrast, Ψ_{ap}^P performs contrastive learning with the guide of the potential consistency between frame-wise temporal and semantic representations. We then compute the inter-information similarity loss \mathcal{L}_{ap}^P between positive pairs below:

$$\mathcal{L}_{ap}^P = \frac{1}{N \cdot T_s} \sum_{i=1}^{N \cdot T_s} (\Psi_{ap}^P[i, i]) \quad (5)$$

where \mathcal{L}_{ap}^P promotes intra-class similarity by considering the one-to-one correspondence between temporal and semantic information, where each frame located at the same position belongs to the same category.

Operations such as random selection [53] or shuffling [29] are usually used to generate negative pairs in the existing works for unsupervised contrastive learning [50], [53], [56], [73]. However, these strategies are usually used for short temporal sequences and they cannot be directly applied to temporal action segmentation due to the complex and various actions in long videos. Here, we further exploit two types of complementary information i.e., temporal and semantic representations to create negative pairs for uncovering their differences. Different from learning inter-information similarity without any auxiliary label information shown in Eq. (4), the construction of negative pairs relies on the results of K-means clustering. Specifically, we can choose pairwise frames with different clustering labels, followed by contrasting these frames. For the t -frame in \mathbf{V}_s , the clustering label generated by K-means can be denoted as $l_{in}[t]$. We can further obtain a matrix, i.e., \mathbf{M}_{in} , which consists of the similarity between any two frames. Regarding the matrix \mathbf{M}_{in} , we have:

$$\mathbf{M}_{in}[i, j] = \begin{cases} 1, & l_{in}[i] = l_{in}[j], \forall i, j \in \{1, 2, \dots, N \cdot T_s\} \\ 0, & \text{other} \end{cases} \quad (6)$$

where \mathbf{M}_{in} indicates the similarity between all sampled frames in a mini-batch. When the clustering labels between the i -th

and j -th frames are identical, the corresponding element in the matrix is set to 1; otherwise, it is set to 0.

The clustering results on the standard input features \mathbf{V}_s cannot be updated during training [25], which may lead to accumulation errors caused by incorrect negative pairs. To reduce these errors, we perform the clustering on the sampled input \mathbf{V}_s , temporal \mathbf{X}_s and semantic \mathbf{H}_s features simultaneously for dynamic selection of potential negative pairs. Hence, we obtain \mathbf{M}_{te} and \mathbf{M}_{se} for \mathbf{X}_s and \mathbf{H}_s , respectively. By combining the three matrices, we generate a matrix $\mathbf{M} \in \mathbb{R}^{N \cdot T_s \times N \cdot T_s}$ that is used to dynamically guide the dissimilarity learning on the negative pairs, defined as:

$$\mathbf{M} = (1 - \mathbf{M}_{in}) \odot (1 - \mathbf{M}_{te}) \odot (1 - \mathbf{M}_{se}) \quad (7)$$

where each element $\mathbf{M}[i, j] \in \{0, 1\}$ represents whether the i -th and j -th frames share the same clustering category. 1 indicates frames from different categories while 0 indicates frames from the same category. The combination of these three matrices can help improve the quality of negative pairs.

Afterwards, we can construct a set of dense negative pairs for each frame based on \mathbf{M} , and negative pairs must be separate. Hence, similar to Eq. (4), the function Ψ_{ap}^N to be minimised with the corresponding inter-information dissimilarity loss \mathcal{L}_{ap}^N is expressed as:

$$\Psi_{ap}^N = - \left[\log \left(\sigma(-\mathbf{H}_s^\top \mathbf{X}_s / \xi) \right) \right] \odot \mathbf{M} \quad (8)$$

$$\mathcal{L}_{ap}^N = \frac{1}{N_{ap}} \sum_{i=1}^{N \cdot T_s} \sum_{j=1}^{N \cdot T_s} (\Psi_{ap}^N[i, j]) \quad (9)$$

where \mathbf{M} is utilised to select pairwise frames between temporal and semantic information to construct inter-information negative pairs. $N_{ap} = \sum_{i=1}^{N \cdot T_s} \sum_{j=1}^{N \cdot T_s} (\mathbf{M}[i, j])$ denotes the number of all the negative pairs. \mathcal{L}_{ap}^N facilitates the separation of inter-information different categories.

Intra-information variation learning. \mathcal{L}_{ap}^P and \mathcal{L}_{ap}^N defined in Eqs. (5) and (9) encourage the temporal model to focus on inter-information variations (i.e., similarity and dissimilarity). Although they implicitly learn the dissimilarity between frames with the semantic or temporal representation, the discriminability of the learned representations is still weak as the inherent discriminative cues within semantic or temporal information are not exploited (this can be verified in Section IV-C1).

Therefore, we further explore the intra-information variations, including the dissimilarities within the semantic or temporal representation. In detail, for each frame of semantic representation (anchor), we choose all the other frames with different clustering labels to form a set of dense intra-information negative pairs. The intra-information dissimilarity loss based on semantic representation \mathbf{H}_s can be computed as:

$$\Psi_{aa}^N = - \left[\log \left(\sigma(-\mathbf{H}_s^\top \mathbf{H}_s / \xi) \right) \right] \odot \mathbf{M} \quad (10)$$

$$\mathcal{L}_{aa}^N = \frac{1}{N_{ap}} \sum_{i=1}^{N \cdot T_s} \sum_{j=1}^{N \cdot T_s} (\Psi_{aa}^N[i, j]) \quad (11)$$

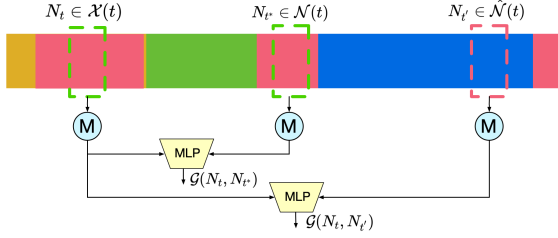


Fig. 4. Illustration of the proposed Neighbourhood-Consistency-Aware Unit. We randomly sample a frame t , and its neighbourhood is N_t (left green dashed box). Then we can use frame t^* with the same label to form the neighbourhood N_{t^*} . The two neighbourhoods are fed into the max-pooling layer to encode their feature distributions, followed by predicting the probability of having similar feature distributions by the MLP model. The same operation is applied to N_t and $N_{t'}$ centered at frames t and t' with different labels.

where σ is the sigmoid function. \mathbf{M} , ξ and N_{ap} are defined in Eqs. (7), (4) and (9), respectively. Here \mathbf{M} is used to select pairwise frames with distinct categories from semantic representation \mathbf{H}_s . \mathcal{L}_{aa}^N encourages the separation of different categories within semantic information. Additionally, we consider the dissimilarity between frames of temporal representation \mathbf{X}_s (positive), and the corresponding loss is defined as follows:

$$\Psi_{pp}^N = -\left[\log\left(\sigma\left(-\mathbf{X}_s^\top \mathbf{X}_s / \xi\right)\right)\right] \odot \mathbf{M} \quad (12)$$

$$\mathcal{L}_{pp}^N = \frac{1}{N_{ap}} \sum_{i=1}^{N \cdot T_s} \sum_{j=1}^{N \cdot T_s} (\Psi_{pp}^N[i, j]) \quad (13)$$

By integrating inter-information losses (i.e., Eqs. (5) and (9)) with the intra-information losses in Eqs. (11) and (13), our proposed semantic-guided multi-level contrast loss is formulated as:

$$\mathcal{L}_{smc} = \mathcal{L}_{ap}^P + \mathcal{L}_{ap}^N + \mathcal{L}_{aa}^N + \mathcal{L}_{pp}^N \quad (14)$$

Notably, by introducing semantic information to the temporal-semantic contrast framework, our method mines more useful information in a large number of unlabelled untrimmed videos. Semantic information plays a multifaceted role in our method: (1) It contributes to the construction of inter-information positive pairs by aligning temporal and semantic information directly, thereby enlarging the intra-class similarity between the two types of information. (2) It also participates in constructing inter-information negative pairs, aiming to enlarge inter-class dissimilarity between the two types of information. (3) It is involved in constructing intra-information negative pairs, further enlarging the intra-class dissimilarity within semantic information. In summary, with the support of semantic information, our SMC can learn representations that capture both the temporal dynamics and semantic nuances of actions, thereby improving the discriminability and robustness of these representations.

D. Neighbourhood-Consistency-Aware Unit

Similar to [25], after having trained the unsupervised model (T : S) by our SMC, we perform semi-supervised learning

for frame-wise classification of temporal actions using few labelled data, as shown in Fig. 3(b). Although this method enjoys good frame-wise accuracy, it suffers from significant over-segmentation errors, leading to low segmentation quality, as measured by segmental F1 score and Edit distance. The reason for this discrepancy lies in the fact that the pre-trained model focuses more on frame-level classification and does not consider the consistency of class labels within an action segment. Over-segmentation refers to the error type where a video is excessively divided into subsegments, causing erratic action class predictions. To alleviate this issue in semi-supervised settings, we introduce a Neighbourhood-Consistency-Aware (NCA) module shown in Fig. 4 to ensure spatial consistency between action segments. The intuition behind this is that feature distribution within the neighbourhoods of the same label should be spatially close.

Concretely, at the first stage shown in Fig. 3(b), given the temporal representation \mathbf{X} of a video with ground-truth labels l in the batch, we randomly sample K frames and construct K neighbourhoods centered at these frames. For each frame, we then select M frames having the same label and M frames with different labels, respectively. Formally, we define the sets of neighbourhoods as:

$$\begin{aligned} \mathcal{X}(t) &= \left\{ N_t = \mathbf{X}\left[t - \frac{W}{2}, t + \frac{W}{2}\right] \mid t \in \mathcal{Z}(t) \right\} \\ \mathcal{N}(t) &= \left\{ N_{t^*} = \mathbf{X}\left[t^* - \frac{W}{2}, t^* + \frac{W}{2}\right] \mid t^* \in \mathcal{P}(t) \right\} \\ \hat{\mathcal{N}}(t) &= \left\{ N_{t'} = \mathbf{X}\left[t' - \frac{W}{2}, t' + \frac{W}{2}\right] \mid t' \in \hat{\mathcal{P}}(t) \right\} \end{aligned} \quad (15)$$

where W is the length of an action segment. $\mathcal{N}(t)$ represents a set of M segments, where each segment consisting of W frames is centered at one frame from a group of M frames. The M frames are randomly sampled from the video frames that have the same label as the frame t . For $\hat{\mathcal{N}}(t)$, M frames are randomly sampled from the video frames that have different labels from frame t . $\mathcal{Z}(t) = \{t_i \mid 1 \leq i \leq K\}$ represents the indices of the sampled K frames. $\mathcal{P}(t) = \{t^* \mid l[t^*] = l[t], \frac{W}{2} \leq t^* \leq T - \frac{W}{2}\}$ and $\hat{\mathcal{P}}(t) = \{t^* \mid l[t^*] \neq l[t], \frac{W}{2} \leq t^* \leq T - \frac{W}{2}\}$ denotes the indices of the frames with the same and different labels corresponding to the t -th frame, respectively.

Our NCA module aims at detecting the inter-neighbourhood consistency, where N_t and N_{t^*} tend to have similar feature distributions, whereas the distributions of N_t and $N_{t'}$ may be different. We define the problem of consistency detection as minimisation practice:

$$\begin{aligned} \mathcal{L}_{nca} &= -\mathbb{E}_{N_t \sim \mathcal{X}(t)} \left[\mathbb{E}_{N_{t^*} \sim \mathcal{N}(t)} [\log \mathcal{G}(N_t, N_{t^*})] \right. \\ &\quad \left. + \mathbb{E}_{N_{t'} \sim \hat{\mathcal{N}}(t)} [\log (1 - \mathcal{G}(N_t, N_{t'}))] \right] \end{aligned} \quad (16)$$

where \mathbb{E} represents the expectation. $\mathcal{G}(N_t, N_{t^*})$ results in the probability of the neighbourhoods having similar feature distributions, formulated as follows:

$$\mathcal{G}(N_t, N_{t^*}) = \mathbf{G}([\max(N_t); \max(N_{t^*})]) \quad (17)$$

where \mathbf{G} is a MLP block (input dimension is $2D$, output dimension is 1) similar to \mathbf{S} in Eq. (3). $[\cdot]$ represents the concatenation operation. $\max(\cdot)$ means max-pooling used to aggregating temporal features [74], [75].

Algorithm 1 The learning process of our SMC-NCA framework.

Input: Input features \mathbf{V} , temporal representation \mathbf{X} and semantic representation \mathbf{H} . Line 2-Line 10: initial unsupervised learning. Line 12-Line 20: semi-supervised learning (stage 1). Line 21-Line 26: semi-supervised learning (stage 2).

```

1: Generate sampled  $\mathbf{V}_s, \mathbf{X}_s$  and  $\mathbf{H}_s$ 
2: for epoch  $e \leftarrow 1$  to E1 do
3:    $\mathcal{L}_{ap}^P \leftarrow -\text{Sum}\left(\left[\log\left(\sigma\left(\mathbf{H}_s^\top \mathbf{X}_s/\xi\right)\right)\right] \odot \mathbf{I}\right) / \text{Sum}(\mathbf{I})$ 
4:    $\mathbf{M} \leftarrow \text{Cluster}(\mathbf{V}_s, \mathbf{X}_s, \mathbf{H}_s)$ 
5:    $\mathcal{L}_{ap}^N \leftarrow -\text{Sum}\left(\left[\log\left(\sigma\left(-\mathbf{H}_s^\top \mathbf{X}_s/\xi\right)\right)\right] \odot \mathbf{M}\right) / \text{Sum}(\mathbf{M})$ 
6:    $\mathcal{L}_{aa}^N \leftarrow -\text{Sum}\left(\left[\log\left(\sigma\left(-\mathbf{H}_s^\top \mathbf{H}_s/\xi\right)\right)\right] \odot \mathbf{M}\right) / \text{Sum}(\mathbf{M})$ 
7:    $\mathcal{L}_{pp}^N \leftarrow -\text{Sum}\left(\left[\log\left(\sigma\left(-\mathbf{X}_s^\top \mathbf{X}_s/\xi\right)\right)\right] \odot \mathbf{M}\right) / \text{Sum}(\mathbf{M})$ 
8:    $\mathcal{L}_{smc} \leftarrow \mathcal{L}_{ap}^P + \mathcal{L}_{ap}^N + \mathcal{L}_{aa}^N + \mathcal{L}_{pp}^N$  (on  $\mathcal{D}$ )
9:   Minimize  $\mathcal{L}_{smc}$  and update models  $\mathbf{T}$  and  $\mathbf{S}$ 
10: end for
11: Obtain the best model evaluated by the linear classifier
12: for iter  $i \leftarrow 1$  to  $I$  do
13:   for epoch  $e \leftarrow 1$  to E2 do
14:      $\mathbf{M} \leftarrow \text{GT}$ 
15:      $\mathcal{L}_{smc} \leftarrow \mathcal{L}_{ap}^P + \mathcal{L}_{ap}^N + \mathcal{L}_{aa}^N + \mathcal{L}_{pp}^N$  (on  $\mathcal{D}_L$ )
16:     Sample  $t \in \mathcal{Z}(t) = \{t_i | 1 \leq i \leq K\}$ 
17:      $\mathcal{L}_{nca} \leftarrow \text{NCA}(t)$ 
18:      $\mathcal{L} \leftarrow \mathcal{L}_{smc} + \mathcal{L}_{nca} + \mathcal{L}_{ce}$ 
19:     Minimize  $\mathcal{L}$  and update models  $\mathbf{T}, \mathbf{S}, \mathbf{G}$  and  $\mathbf{C}$ 
20:   end for
21:   for epoch  $e \leftarrow 1$  to E3 do
22:      $\text{PL} \leftarrow \mathbf{C}(\mathcal{D}_U)$ 
23:      $\mathbf{M} \leftarrow \text{PL} \cup \text{GT}$ 
24:      $\mathcal{L} \leftarrow \mathcal{L}_{smc} + \mathcal{L}_{nca}$  (on  $\mathcal{D}$ )
25:     Minimize  $\mathcal{L}$  and update models  $\mathbf{T}, \mathbf{S}$  and  $\mathbf{G}$  on  $\mathcal{D}$ 
26:   end for
27: end for

```

The loss function can be approximated as:

$$\mathcal{L}_{nca} = -\frac{1}{K \times M} \sum_{i=1}^K \sum_{j=1}^M \left[\log \mathcal{G}(N_t^i, N_{t'}^j) + \log(1 - \mathcal{G}(N_t^i, N_{t'}^j)) \right] \quad (18)$$

At this stage, our SMC is guided by ground-truth labels of labelled videos. Thus, the overall loss is defined as $\mathcal{L} = \mathcal{L}_{smc} + \mathcal{L}_{nca} + \mathcal{L}_{ce}$, where \mathcal{L}_{ce} is the standard frame-level cross-entropy for action classification:

$$\mathcal{L}_{ce} = -\frac{1}{T} \sum_{t=1}^T \sum_{a=1}^A y_a[t] \log(\hat{y}_a[t]) \quad (19)$$

where $\hat{y}_a[t]$ represents the predicted probability of the t -th frame belonging to class a . At the second stage, the ground-truth labels are combined with the pseudo labels (PL) generated by \mathbf{C} at the first stage to guide the learning of \mathbf{T} ,

\mathbf{S} and \mathbf{G} for further updating frame-level representation. Our SMC-NCA framework is summarised in Algorithm 1.

IV. EXPERIMENTS

A. Datasets and Evaluation

Public Action Segmentation Datasets. We evaluate the proposed method on three challenging datasets: **50Salads** [76] (50 videos, 19 actions), **GTEA** [77] (28 videos, 11 actions), and **Breakfast Actions** [78] (1712 videos, 10 complex activities, 48 actions). Following [25], we use the standard train-test splits for each dataset.

Mouse Social Behaviour Dataset. Based on the dataset from our previous works [79]–[82], we introduce a new Parkinson’s Disease Mouse Behaviour (PDMB) dataset consisting of three groups of normal mice and three groups of mice with Parkinson’s Disease. It provides a valuable resource to study the behavioural patterns and characteristics of mice, particularly those with Parkinson’s Disease. More details can be found in Supplementary B.

Evaluation. We follow the evaluation protocol used in ICC [25] for both unsupervised and semi-supervised settings. In specific, for the public datasets, we use the same evaluation metrics taken for fully-supervised temporal action segmentation, including frame-wise accuracy (Acc), segmental Edit distance (Edit), and segmental F1 score at overlapping thresholds 10%, 25%, and 50% (denoted as $\text{F1}@_{\{10, 25, 50\}}$) [6]. The overlapping ratio is the intersection over union (IoU) ratio between the predicted and ground-truth action segments. We conduct cross-validation using the standard splits [25], and report the average. We evaluate the representation generated in unsupervised learning by training a linear classifier to classify frame-wise action labels. In the semi-supervised setting, we also report the average of 5 different selections to reduce the randomness brought by the training subset selection. For our PDMB dataset, we also use similar evaluation metrics and define 2 splits for cross-validation.

B. Implementation Details.

All our experiments are performed on Nvidia Tesla P100 GPUs with 16GB memory. The parameters are optimised by the Adam algorithm. Learning Rate (LR), Weight Decay (WD), Epochs (Eps), and Batch Size (BS) used for our unsupervised and semi-supervised setups can be found in Tab. S2. Similar to [25], the number of iterations is set to 4. Following the default of ICC [25], we set the number of clusters in K-means to 40, 30 and 100 for 50Salads, GTEA and Breakfast datasets, respectively. At the beginning of unsupervised representation learning, ξ is set to 1 for 50salads, GTEA and our PDMB dataset, and 0.1 for the large dataset Breakfast. In the NCA module, the length of a neighbourhood W , the number of the selected frames K , and the number of frames M with the same label for each selected frame are set to 8, 1 and 10, respectively. The source code will be published after the paper has been accepted.

TABLE I
COMPONENT-WISE ANALYSIS OF THE UNSUPERVISED REPRESENTATION LEARNING FRAMEWORK WITH A LINEAR CLASSIFIER.

Method	50Salads					GTEA				
	F1@{10, 25, 50}			Edit	Acc	F1@{10, 25, 50}			Edit	Acc
$\mathcal{L}_{ap}^P(\mathbf{M}_{in})+\mathcal{L}_{aa}^N$	36.8	31.1	22.6	29.8	57.1	73.1	66.3	48.5	65.5	70.2
$\mathcal{L}_{ap}^P(\mathbf{I})+\mathcal{L}_{aa}^N$	51.9	46.8	38.2	39.7	72.4	75.8	71.1	53.0	68.0	73.8
$\mathcal{L}_{ap}^P(\mathbf{M}_{in})+\mathcal{L}_{ap}^N$	39.1	33.8	25.2	31.8	56.4	69.8	63.7	48.3	64.3	68.8
$\mathcal{L}_{ap}^P(\mathbf{I})+\mathcal{L}_{ap}^N$	40.7	35.6	26.4	30.9	64.8	73.0	67.6	50.0	66.1	70.8
<i>Constructing positive pairs by \mathbf{M}_{in} (rely on the clustering results) or \mathbf{I} (without relying on the clustering)</i>										
$\mathcal{L}_{ap}^P + \mathcal{L}_{aa}^N$	51.9	46.8	38.2	39.7	72.4	75.8	71.1	53.0	68.0	73.8
$\mathcal{L}_{ap}^P + \mathcal{L}_{ap}^N$	40.7	35.6	26.4	30.9	64.8	73.0	67.6	50.0	66.1	70.8
$\mathcal{L}_{ap}^P + \mathcal{L}_{aa}^N + \mathcal{L}_{ap}^N$	55.2	50.1	42.0	44.0	73.1	76.2	71.8	55.7	67.9	75.0
$\mathcal{L}_{ap}^P + \mathcal{L}_{aa}^N + \mathcal{L}_{ap}^N + \mathcal{L}_{pp}^N$	56.5	52.1	42.8	45.4	74.3	77.4	71.2	56.1	69.0	75.7
<i>Comparing different negative pairs</i>										
w/o dynamic clustering	56.5	52.1	42.8	45.4	74.3	77.4	71.2	56.1	69.0	75.7
w/ dynamic clustering	58.1	54.0	43.5	46.3	75.1	78.9	74.3	59.2	73.0	76.2
<i>Dynamic clustering facilitates contrastive learning</i>										

C. Ablation Studies

1) *Evaluation of Representation Learning: Effect of positive pairs construction.* As defined in Eq. (4), we construct the positive pairs based on the inherent similarity between frame-wise representations with temporal and semantic information rather than matrix, e.g., \mathbf{M}_{in} from the clustering outcomes. Tab. I (Top) shows the impact of positive pair construction for the inter-information similarity learning on two public datasets (i.e., 50Salads and GTEA datasets). We replace \mathbf{I} in Eq. (4) with \mathbf{M}_{in} to generate dense positive pairs, and the corresponding loss $\mathcal{L}_{ap}^P(\mathbf{M}_{in})$ is combined with \mathcal{L}_{aa}^N and \mathcal{L}_{ap}^N respectively for representation learning. As shown in Tab. I (Top), we experience a significant decrease in performance using the contrastive learning guided by \mathbf{M}_{in} , especially on the 50Salads dataset. This is likely caused by the fact that this design results in more clustering errors, thus affecting inter-information similarity learning.

TABLE II
ABLATION STUDY ON THE BREAKFAST DATASET.

Method	Breakfast				
	F1@{10, 25, 50}			Edit	Acc
$\mathcal{L}_{ap}^P + \mathcal{L}_{aa}^N$	57.4	52.6	39.0	51.0	70.3
$\mathcal{L}_{ap}^P + \mathcal{L}_{ap}^N$	56.3	51.2	38.4	50.3	69.1
$\mathcal{L}_{ap}^P + \mathcal{L}_{aa}^N + \mathcal{L}_{ap}^N$	58.2	54.1	41.0	52.1	71.7
$\mathcal{L}_{ap}^P + \mathcal{L}_{aa}^N + \mathcal{L}_{ap}^N + \mathcal{L}_{pp}^N$	59.0	54.0	41.9	52.2	71.9
w/o dynamic clustering	59.0	54.0	41.9	52.2	71.9
w/ dynamic clustering	59.7	55.4	42.8	52.7	72.1

TABLE III
COMPARING SEMANTIC FEATURE EXTRACTORS ON THE 50SALADS DATASET.

Method	F1@{10, 25, 50}			Edit	Acc
MLP (1 layer)	58.1	54.0	43.5	46.3	75.1
MLP (3 layers)	45.4	41.0	32.5	37.3	61.9
MLP (5 layers)	39.4	34.6	25.1	32.3	57.6
Conv1d (1 layers)	55.1	50.0	41.0	44.1	72.0
Conv1d (3 layers)	42.7	38.6	28.1	34.6	59.3
Conv1d (5 layers)	37.9	32.5	22.9	31.4	54.1

Effect of negative pairs construction. Tab. I (Middle) illustrates the results of the combinations of loss functions. In our SMC framework, we construct three types of dense

negative pairs from the representations with temporal, semantic information and their combinations, respectively (the corresponding losses can be annotated as \mathcal{L}_{pp}^N , \mathcal{L}_{aa}^N and \mathcal{L}_{ap}^N). As shown in Tab. I (Middle), compared with \mathcal{L}_{ap}^N , \mathcal{L}_{aa}^N achieves better F1 and Edit scores and accuracy, with improvements of around 10% and 3% on the 50Salads and GTEA datasets. This demonstrates that contrasting learning using semantic representations enables effective dissimilarity learning between frames. In addition, using \mathcal{L}_{aa}^N with \mathcal{L}_{ap}^N brings significant gains in all the metrics on the 50Salads and GTEA datasets, showing that these two losses are complementary to enhance contrastive learning as they impose intra- and inter-information dissimilarity learning, respectively. We further observe that the overall performance is slightly improved on both datasets by adding the contrastive loss with temporal representation, i.e., \mathcal{L}_{pp}^N . On the Breakfast dataset, we can also achieve the best performance for all metrics by combining three types of negative pairs at the same time. The results are reported in Tab. II. We also study the training process using different loss functions, as shown in Fig. 5. As training progresses, the approach with three loss functions constantly outperforms the other approaches.

Effect of dynamic clustering. As described in Section III-C, we exploit the dynamic matrix \mathbf{M} in Eq. (7) to guide multi-level contrast. Tab. I (Bottom) and Tab. II (Bottom) show the effect of dynamic clustering. Note that the method without dynamic clustering refers to the approach with the fixed matrix \mathbf{M}_{in} . From Tab. I (Bottom) and Tab. II (Bottom), we discover that the segmentation performance can be further improved by applying the dynamic clustering to the selection of negative pairs. This is mainly because dynamic clustering allows us to further reduce the clustering errors by joint clustering on the temporal, semantic and pre-trained input features.

Effect of different semantic feature extractors. Tab. III shows the results of using different semantic feature extractors for constructing multi-level contrastive learning. Semantic features provide context about the scene or objects present in the video frames, which highlights action-specific attributes. First, they assist in creating inter-information positive pairs to reinforce intra-class similarity. For instance, frames at corresponding positions in the sequence, both in terms of semantic

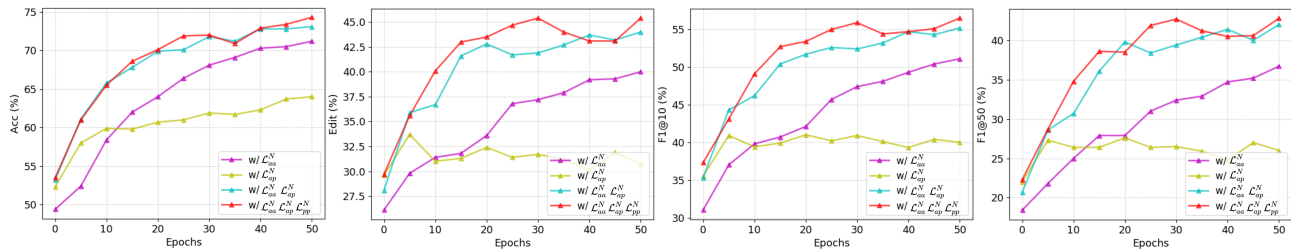


Fig. 5. Performance of unsupervised representation learning using different loss functions during training on 50Salads.

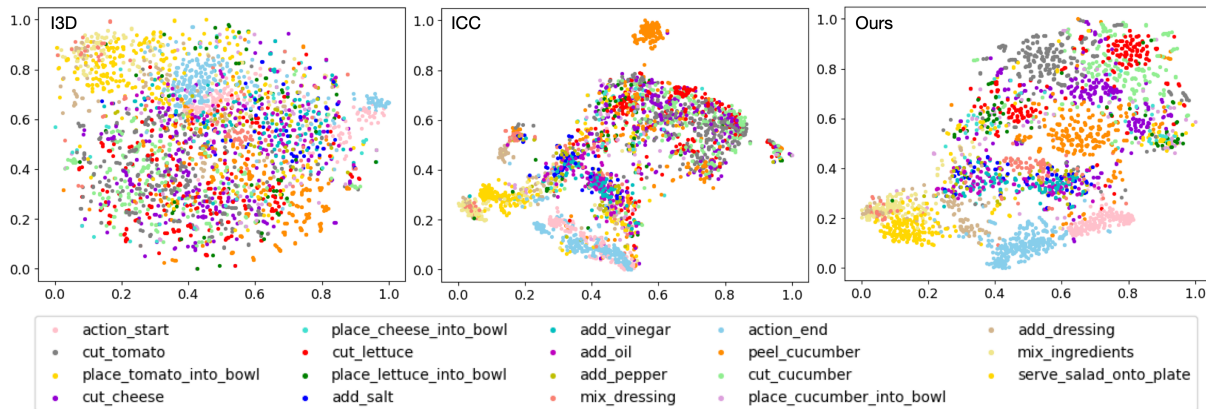


Fig. 6. t-SNE visualisation of the I3D feature and other features learned by ICC and our method. Each point represents an image frame. We show all action classes (19) of the 50Salads dataset in different colours.

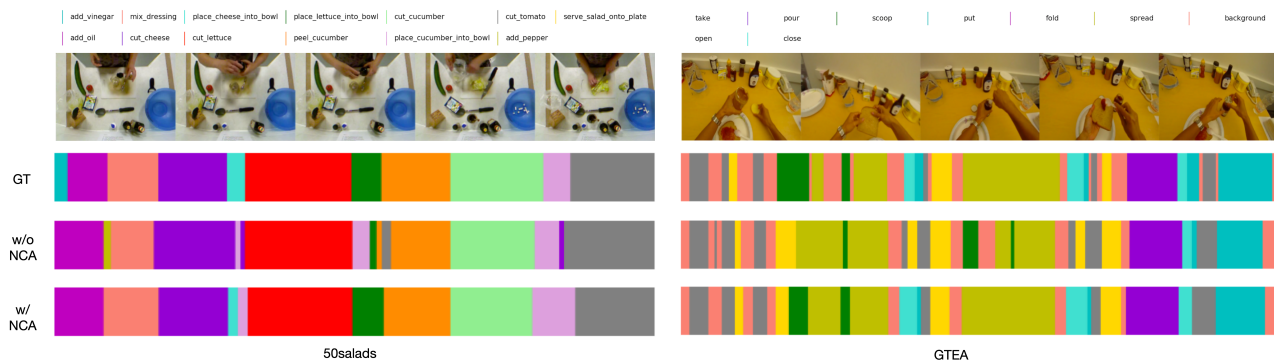


Fig. 7. Qualitative visualisation of segmentation results on the 50Salads and GTEA datasets with 5% labelled data.

and temporal features, are expected to belong to the same action category. Second, they contribute to enlarging inter-class dissimilarity by constructing inter-information negative pairs and intra-information negative pairs, respectively. ‘MLP (1 layer)’ means a single-layer MLP, which has one hidden layer between the input and output layers. ‘Conv1d’ refers to a one-dimensional convolutional layer. We can observe that greater complexity of semantic feature extractors may lead to worse performance. Therefore, we choose MLP (1 layer) as the semantic feature extractor.

Qualitative Results. In this section, we employ t-Distributed Stochastic Neighbor Embedding (t-SNE) to visualise the I3D feature alongside other features learned by ICC and our proposed method on the 50Salads dataset, as shown in Fig. 6. Each colour in the figure corresponds to

a distinct action. The features selected for visualisation are randomly sampled from the combined multi-resolution representation extracted by the C2F-TCN model [25]. Notably, our method exhibits superior class separation, indicating the strong representation learning capability facilitated by our Semantic-guided Multi-level Contrast scheme. This enhanced separation shows the effectiveness of our approach in capturing more discriminative representation for action segmentation.

2) *Evaluation of Semi-supervised Learning: Effect of the NCA unit.* In Section III-D, we propose the NCA module to alleviate over-segmentation issues when only a fraction of videos are used for semi-supervised learning. Tab. V shows the results where only 5% of labelled videos are used for semi-supervised learning on the 50Salads, GTEA and Breakfast datasets. While the baseline without \mathcal{L}_{nca} achieves the

TABLE IV
COMPARING OUR PROPOSED SEMI-SUPERVISED APPROACH WITH THE SUPERVISED LEARNING APPROACH USING THE SAME LABELLED DATA ON THE 3 BENCHMARK DATASETS.

%D _L	Method	50salads					GTEA					Breakfast				
		F1@{10, 25, 50}					F1@{10, 25, 50}					F1@{10, 25, 50}				
5	Supervised	30.5	25.4	17.3	26.3	43.1	64.9	57.5	40.8	59.2	59.7	15.7	11.8	5.9	19.8	26.0
	Semi-Super	57.0	53.1	42.1	48.9	68.9	81.9	79.3	64.0	77.9	73.9	62.7	57.0	41.6	60.2	68.9
	Gain	26.5	27.7	24.8	22.6	25.8	17.0	21.8	23.2	18.7	14.2	47.0	45.2	35.7	40.4	42.9
10	Supervised	45.1	38.3	26.4	38.2	54.8	66.2	61.7	45.2	62.5	60.6	35.1	30.6	19.5	36.3	40.3
	Semi-Super	70.3	66.3	54.7	61.3	73.6	87.7	84.2	71.7	83.3	77.5	64.8	60.2	45.0	63.4	69.7
	Gain	25.2	28.0	28.3	23.1	18.8	21.5	22.5	26.5	20.8	16.9	29.7	29.6	25.5	27.1	29.4
100	Supervised	75.8	73.1	62.3	68.8	79.4	90.1	87.8	74.9	86.7	79.5	69.4	65.9	55.1	66.5	73.4
	Semi-Super	86.9	84.8	78.9	80.7	87.0	92.7	91.0	81.5	88.3	82.6	73.8	69.7	56.8	70.9	76.4
	Gain	11.1	11.7	16.6	11.9	7.6	2.6	3.2	6.6	1.6	3.1	4.4	3.8	1.7	4.4	3.0

TABLE V
PERFORMANCE OF THE NCA MODULE ON THE 50SALADS, GTEA AND BREAKFAST DATASETS (5%).

Dataset	Method	F1@{10, 25, 50}				
50Salads	w/o \mathcal{L}_{nca}	52.1	47.0	35.8	43.9	67.5
	w/ \mathcal{L}_{nca}	57.0	53.1	42.1	48.9	68.9
	Gain	4.9	6.1	6.3	5.0	1.4
GTEA	w/o \mathcal{L}_{nca}	77.5	74.2	57.7	71.8	71.4
	w/ \mathcal{L}_{nca}	81.9	79.3	64.0	77.9	73.9
	Gain	4.4	5.1	6.3	6.1	2.5
Breakfast	w/o \mathcal{L}_{nca}	60.8	54.8	39.5	58.1	68.1
	w/ \mathcal{L}_{nca}	62.7	57.0	41.6	60.2	68.9
	Gain	1.9	2.2	1.1	2.1	0.8

TABLE VI
COMPARING OUR PROPOSED UNSUPERVISED REPRESENTATION LEARNING APPROACH WITH OTHER EXISTING METHODS ON THE 3 BENCHMARKS.

Dataset	Method	F1@{10, 25, 50}				
50Salads	I3D	12.2	7.9	4.0	8.4	55.0
	ICC [25]	40.8	36.2	28.1	32.4	62.5
	SMC	58.1	54.0	43.5	46.3	75.1
	Gain	17.3	17.8	15.4	13.9	12.6
GTEA	I3D	48.5	42.2	26.4	40.2	61.9
	ICC [25]	70.8	65.0	48.0	65.7	69.1
	SMC	78.9	74.3	59.2	73.0	76.2
	Gain	8.1	9.3	11.2	7.3	7.1
Breakfast	I3D	4.9	2.5	0.9	5.3	30.2
	ICC [25]	57.0	51.7	39.1	51.3	70.5
	SMC	59.7	55.4	42.8	52.7	72.1
	Gain	2.7	3.7	3.7	1.4	1.6

expected frame-wise accuracy, it suffers from severe over-segmentation as indicated by the low F1 and Edit scores. By incorporating \mathcal{L}_{nca} within the SMC module, we observe a significant performance boost, up to 6.1% improvement for the Edit score, and up to 6.3% improvement for the F1 score on the 50 Salads and GTEA. These results show that our proposed NCA module is capable of reducing over-segmentation errors by identifying the spatial consistency between the action segments.

Semi-supervised Vs Supervised. We also compare our proposed semi-supervised approach with the supervised counterpart using the same labelled data on the 3 benchmarks, and the results are reported in Tab. IV. Performance improvement is noticeable over all the evaluation metrics in both semi-supervised (5% and 10%) and fully-supervised (100%) setups, confirming the effectiveness of our semi-supervised learning framework.

Qualitative Results. Qualitative results of the NCA module are presented in Fig. 7. When observing prediction results without the NCA module, we notice certain over-segmentation errors characterised by numerous small segments. However, our NCA effectively alleviates this issue by identifying spatial consistency between neighbourhoods centered at different frames. This demonstrates that our proposed NCA ensures smoother and more coherent segmentation results.

D. Comparison against other State-of-the-Art Approaches

In this section, we compare our proposed unsupervised representation learning and semi-supervised learning framework against the other existing methods on three public datasets, i.e., 50 Salads, GTEA and Breakfast datasets and our PDMB dataset. Tabs. VI and VIII report the results of the unsupervised representation learning and supervised learning with different levels (i.e., fully-, weakly- and semi-supervised) on the three human action datasets. Tabs. XI and XII show the results on our mouse social behaviour dataset.

1) *Comparison on human action datasets:* As shown in Tab. VI, our SMC is superior to the standard ICC in all the metrics, up to 17.8% gain for F1 score, 13.9% gain for Edit score and 12.6% gain for the frame-wise accuracy on the 50 Salads dataset. We observe a similar tendency on the GTEA dataset, with improvements of 11.2%, 7.3% and 7.1% for the F1 score, Edit score and accuracy, respectively. The performance of our SMC is primarily attributed to its ability to capture and exploit intra- and inter-information variations. Regarding the Breakfast dataset with complex activities, we keep the video-level contrastive loss in ICC [25] and combine it with our SMC to ensure a fair comparison. The results in Tab. VI show that our approach is marginally better than ICC for all the evaluation metrics.

In Tab. VIII, we show the implementation results of our semi-supervised method using 100% labelled data, the best frame-wise accuracy among all the fully-supervised approaches. For the semi-supervised setting, we literally perform unsupervised representation learning and semi-supervised classification for 5%, 10% and 40% of the training data, and the results show that our framework consistently outperforms ICC by a significant margin. It is noticed that the performance gap (i.e., 7.6%, 5.7% and 3.6% improvements in accuracy on the three datasets) between the two methods using only 5% labelled videos is larger than that using more labelled

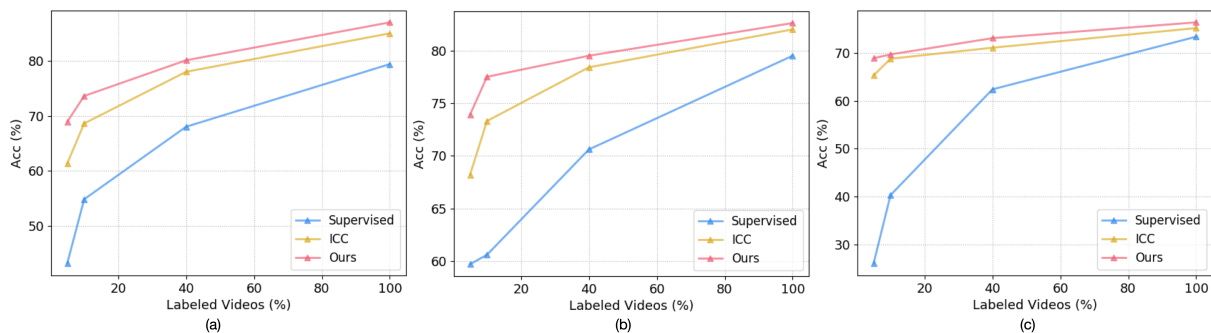


Fig. 8. Segmentation accuracy of different methods on (a) 50Salads, (b) GTEA and (c) Breakfast datasets. Our semi-supervised approach continuously achieves satisfactory performance over semi-supervised (5%, 10% and 40%) and fully-supervised (100%) setups.

TABLE VII
COMPARING OUR PROPOSED SEMI-SUPERVISED APPROACH WITH ICC ON THE 3 BENCHMARKS.

%D _L	Method	50salads					GTEA					Breakfast				
		F1@{10, 25, 50}			Edit	Acc	F1@{10, 25, 50}			Edit	Acc	F1@{10, 25, 50}			Edit	Acc
5	ICC [25]	52.9	49.0	36.6	45.6	61.3	77.9	71.6	54.6	71.4	68.2	60.2	53.5	35.6	56.6	65.3
	Ours (SMC-NCA)	57.0	53.1	42.1	48.9	68.9	81.9	79.3	64.0	77.9	73.9	62.7	57.0	41.6	60.2	68.9
	Gain	4.1	4.1	5.5	3.3	7.6	4.0	7.7	9.4	6.5	5.7	2.5	3.4	6.0	3.6	3.6
10	ICC [25]	67.3	64.9	49.2	56.9	68.6	83.7	81.9	66.6	76.4	73.3	64.6	59.0	42.2	61.9	68.8
	Ours (SMC-NCA)	70.3	66.3	54.7	61.3	73.6	87.7	84.2	71.7	83.3	77.5	64.8	60.2	45.0	63.4	69.7
	Gain	3.0	1.4	5.5	4.4	5.0	4.0	2.3	5.1	6.9	4.2	0.2	1.2	2.8	1.5	0.9
40	ICC [25]					78.0					78.4					71.1
	Ours (SMC-NCA)	76.5	73.6	65.6	67.9	80.1	85.8	83.6	72.8	80.2	79.5	69.0	64.2	49.5	67.1	73.1
	Gain					2.1					1.1					2.0
100	ICC [25]	83.8	82.0	74.3	76.1	85.0	91.4	89.1	80.5	87.8	82.0	72.4	68.5	55.9	68.6	75.2
	Ours	86.9	84.8	78.9	80.7	87.0	92.7	91.0	81.5	88.3	82.6	73.8	69.7	56.8	70.9	76.4
	Gain	3.1	2.8	4.6	4.6	2.0	1.3	1.9	1.0	0.5	0.6	1.4	1.2	0.9	2.3	1.2

TABLE VIII
SEGMENTATION ACCURACY COMPARISON AGAINST THE STATE-OF-THE-ART METHODS UNDER VARIOUS SUPERVISIONS ON 3 BENCHMARK DATASETS.

	Method	50Salads	GTEA	Breakfast
Fully	MSTCN [15]	83.7	78.9	67.6
	SSTDA [83]	83.2	79.8	70.2
	C2F-TCN [33]	79.4	79.5	73.4
	ASFormer [16]	85.6	79.7	73.5
	CETNet [84]	86.9	80.3	74.9
	DiffAct [85]	88.9	82.2	76.4
	ICC [25] (100%)	85.0	82.0	75.2
	Ours (SMC-NCA)(100%)	87.0	82.6	76.4
	Weakly	SSTDA [83] (65%)	80.7	75.7
Timestamp [24]		75.6	66.4	64.1
Semi	ICC [25] (40%)	78.0	78.4	71.1
	Ours (SMC-NCA)(40%)	80.1	79.5	73.1
	ICC [25] (10%)	68.6	73.3	68.8
	Ours (SMC-NCA)(10%)	73.6	77.5	69.7
	ICC [25] (5%)	61.3	68.2	65.3
Ours (SMC-NCA)(5%)	68.9	73.9	68.9	

data. This confirms that our approach is capable of dealing with semi-supervised learning problems in the presence of a small amount of labelled data. As shown in Tab. VII and Fig. 8, we evaluate our method on three benchmarks and achieve continuously better results for all the performance measures.

We have compared our method with ICC (the most relevant to our work) in Tab. VIII. Regarding another study [26] on semi-supervised temporal action segmentation, since it does not provide publicly available code and implementation

TABLE IX
COMPARISONS AGAINST OTHER SEMI-SUPERVISED LEARNING METHODS ON 5% LABELLED DATA.

Dataset	Method	F1@{10, 25, 50}	Edit	Acc
50Salads	FixMatch [65]	47.0 41.3 28.3	38.3	53.3
	UniMatch [86]	50.3 45.9 30.4	39.7	54.4
	Ours (SMC-NCA)	57.0 53.1 42.1	48.9	68.9
GTEA	FixMatch [65]	69.1 63.9 44.1	59.5	62.0
	UniMatch [86]	65.4 60.0 40.8	57.4	58.7
	Ours (SMC-NCA)	81.9 79.3 64.0	77.9	73.9

details, we are unable to directly compare it with our method. As mentioned in [25], ICC is the first work for semi-supervised action segmentation and is not directly comparable to other works. Most existing image-based semi-supervised learning techniques are not suitable for action segmentation. The reason is that data augmentations (e.g., rotation and transformation) should be applied to input images, but it is non-trivial for action segmentation as the inputs are pre-computed feature vectors [26]. However, we managed to compare our method against two popular semi-supervised learning methods, i.e., FixMatch [65] and UniMatch [86]. In order to reproduce these methods, we designed different data augmentation strategies (e.g., noise) to generate input features with different levels of augmentations. Specifically, for FixMatch, we apply scale transformation (0.2 to 2) for weak augmentation and add Gaussian noise (mean 0, standard deviation 1) [87] for strong augmentation. Similarly, for UniMatch, we use the same approach for weak augmentation and adopt channel dropout

with a probability of 50% as our feature perturbation [86]. Additionally, we add different Gaussian noises (standard deviation 1 and 1.5) for strong augmentations. The results reported in Tab. IX further verify the superiority of our method.

2) *Computational complexity*: To analyse the computational complexity of our proposed SMC-NCA framework, we report the FLOPs and parameter numbers on the 50Salads dataset using an input with the shape $1 \times 2048 \times 960$ (1, 2048 and 960 denote bath size, feature dimension and temporal length), as shown in Tab. X. Specifically, we investigate the computational complexity of three distinct base TCN models, namely ED-TCN [6] (an encoder-decoder architecture) MS-TCN [15] (we only use the single-stage configuration as MS-TCN is not designed for representation learning [25]) and C2F-TCN [25], [27]. To perform semi-supervised learning, we apply the learning strategies proposed in [25] to these models and the results are reported in the first three rows. We can observe that MS-TCN has the fewest parameters and FLOPs, but its segmentation performance is the poorest. One of the reasons can be that MS-TCN does not have multiple temporal resolution representations like encoder-decoder architecture which is important for unsupervised representation learning. Notably, ICC leveraging C2F-TCN emerges as the top performer among the three methods, demonstrating superior segmentation performance at a computational expense less than half of that of ED-TCN.

As mentioned in Sec. III, we construct a novel SMC scheme to boost unsupervised representation learning by introducing a simple semantic feature extractor (single-layer MLP in Tab. III). By applying our SMC to the C2F-TCN backbone of ICC, our proposed approach demonstrates higher computational demands compared to ICC. Specifically, our method with SMC exhibits a notable increase in both FLOPs (from 2.4G to 5.4G) and parameter numbers (from 4.3M to 7.4M). This can be attributed to the addition of the MLP that maps input \mathbf{V} of feature dimension E (i.e., 2048) to output \mathbf{H} of feature dimension D (i.e., 1536). Despite the increased computational cost, our approach achieves superior performance in both unsupervised and semi-supervised settings. Moreover, incorporating the NCA module slightly increases the parameter count by 0.4M while maintaining the same FLOPs (5.4G). However, the overall semi-supervised performance is significantly improved compared to ICC. It is noticeable that our proposed SMC and NCA are exclusively utilised during model training to enhance the semi-supervised segmentation performance of the backbone. Consequently, they do not contribute to any increase in inference time per video.

3) *Comparison on mouse social behaviour dataset*: Temporal dependency modelling is crucial for the detection and segmentation of human actions in long videos [15], [16]. For animal behaviours such as mouse social behaviour recognition in long videos, behavioural correlations are also of importance to infer the social behaviour label of each frame [80]. Therefore, to demonstrate the generalisation and effectiveness of our proposed framework, we conducted experiments on our PDMB dataset. Tab. XI depicts that our proposed SMC outperforms ICC by a large margin, offering an improvement of more than 20% for all metrics on the PDMB dataset. The reason why

TABLE X
ANALYSIS OF COMPUTATIONAL COST ON THE 50SALADS DATASETS IN TERMS OF FLOPS AND PARAMETER NUMBER (PARAMS). THE SEMI-SUPERVISED RESULTS OF EDIT AND ACC ARE BASED ON 5% LABELLED DATA.

Method	FLOPs	Params	Unsupervised		Semi	
			Edit	Acc	Edit	Acc
ED-TCN [6]	7.3G	8.2M	\	\	32.7	46.4
MS-TCN [15]	0.3G	0.3M	\	\	23.4	38.3
ICC [25]	2.4G	4.3M	32.4	62.5	45.6	61.3
Ours (SMC)	5.4G	7.4M	46.3	75.1	43.9	67.5
Ours (SMC-NCA)	5.4G	7.8M	\	\	48.9	68.9

TABLE XI
COMPARING OUR PROPOSED UNSUPERVISED REPRESENTATION LEARNING APPROACH WITH ICC ON THE PDMB DATASET.

Dataset	Method	F1@{10, 25, 50}			Edit	Acc
PDMB	ICC [25]	37.5	32.5	20.6	35.2	40.1
	SMC	61.1	59.6	47.2	55.3	62.5
	Gain	23.6	27.1	26.6	20.3	22.4

ICC has poor performance is that it only exploits temporal information that encodes temporal dependencies of mouse social behaviours to explore the variations of related frames. However, this approach may lead to suboptimal representation learning performance due to complex and diverse behavioural patterns in long videos. In contrast, our proposed SMC integrates both temporal and semantic information, which encodes the behavioural correlations and behaviour-specific characteristics, respectively. By exploiting the intra- and inter-information variations, our framework is able to learn more discriminative frame-wise representations.

We have also compared our entire framework, i.e., SMC-NCA with ICC using different settings of labelled data on our PDMB dataset. As presented in Tab. XII, our approach achieves superior performance over ICC using only 10%, 50% as well as 100% labelled data, thus demonstrating the effectiveness of our semi-supervised learning framework in modelling behavioural correlations of mice. Notably, the accuracy of our method varies across different datasets, with lower accuracy observed on the mouse behaviour dataset compared to human action datasets. This discrepancy may arise from several factors. First, mouse behaviours are often more complex and variable [80], [82], with shorter durations and more frequent transitions between behaviours, leading to intricate behavioural correlations that are challenging to capture accurately. Second, our proposed method uses a temporal feature extractor originally designed for human action

TABLE XII
COMPARING OUR PROPOSED FRAMEWORK WITH ICC ON THE PDMB DATASET.

%D _L	Method	PDMB				
		F1@{10, 25, 50}			Edit	Acc
10	ICC [25]	50.0	42.5	25.5	49.7	44.5
	Ours (SMC-NCA)	62.0	57.1	40.7	52.7	55.1
50	ICC [25]	63.5	59.5	40.5	54.4	58.6
	Ours (SMC-NCA)	68.0	63.3	46.6	59.0	66.8
100	ICC [25]	68.1	63.1	46.1	59.8	69.4
	Ours (SMC-NCA)	71.7	67.5	51.7	63.0	73.6

segmentation [27]. While effective for human actions, it may not adequately capture the unique features of mouse behaviour due to fundamental differences in movement patterns and action sequences.

Finally, to demonstrate the applicability of the proposed framework to behaviour phenotyping of the mice with Parkinson's disease, we investigate the behavioural correlations of both MPTP-treated mice and their control strains, as shown in Fig. S2. The findings reveal that MPTP-treated mice are more likely to perform 'approach' after 'circle', 'up' or 'walk_away' compared to the control group ('other' is excluded). Besides, MPTP-treated mice tend to exhibit 'sniff' behaviour while the normal mice show a higher propensity towards 'walk_away' after 'chase'.

V. CONCLUSIONS AND FUTURE WORK

We have presented SMC-NCA, a novel semantic-guided multi-level contrast framework that aims to yield more discriminative frame-wise representations by fully exploiting complementary information from semantic and temporal entities. The proposed SMC aims to explore intra- and inter-information variations for unsupervised representation learning by integrating both semantic and temporal information. To achieve this goal, three types of dense negative pairs are explicitly constructed to facilitate contrastive learning. Our SMC provides a comprehensive solution that leverages both semantic and temporal features to enable effective unsupervised representation learning for action segmentation. To alleviate the over-segmentation problems in the semi-supervised setting with only a small amount of labelled data, the NCA module fully utilises spatial consistency between the neighbourhoods centered at different frames. Our framework outperforms the other state-of-the-art approaches on the three public datasets and our PDMB dataset, demonstrating the generalisation and versatility of our proposed framework for datasets of different domains. However, for datasets such as Breakfast, which features video-level activity labels, our multi-level contrast framework needs to be further developed to handle the similarity of activities. We will leave this exploration as future work. In addition, our approach and insights may also apply to other video tasks, particularly those involving long untrimmed videos, such as temporal action detection.

When the amount of labelled data is very limited, such as 5%, the performance of the current contrast-classify framework in a semi-supervised setting can be potentially impacted by the quality of the pseudo labels. To address this, our future work will focus on enhancing the quality of pseudo labels to further improve representation learning. Additionally, we plan to develop more robust temporal and semantic feature extractors and devise methods to more effectively leverage the complementary information between them. By improving both the pseudo label generation process and the feature extraction techniques, we aim to achieve better performance even with minimal labelled data.

REFERENCES

- [1] T. Yu, L. Wang, C. Da, H. Gu, S. Xiang, and C. Pan, "Weakly semantic guided action recognition," *IEEE Transactions on Multimedia*, vol. 21, no. 10, pp. 2504–2517, 2019. 1
- [2] S. Liu and X. Ma, "Attention-driven appearance-motion fusion network for action recognition," *IEEE Transactions on Multimedia*, vol. 25, pp. 2573–2584, 2023. 1
- [3] M. Moniruzzaman, Z. Yin, Z. He, R. Qin, and M. C. Leu, "Human action recognition by discriminative feature pooling and video segment attention model," *IEEE Transactions on Multimedia*, vol. 24, pp. 689–701, 2022. 1
- [4] Y. Kong, Y. Wang, and A. Li, "Spatiotemporal saliency representation learning for video action recognition," *IEEE Transactions on Multimedia*, vol. 24, pp. 1515–1528, 2022. 1
- [5] J. Wang, Y. Lin, M. Zhang, Y. Gao, and A. J. Ma, "Multi-level temporal dilated dense prediction for action recognition," *IEEE Transactions on Multimedia*, vol. 24, pp. 2553–2566, 2022. 1
- [6] C. Lea, M. D. Flynn, R. Vidal, A. Reiter, and G. D. Hager, "Temporal convolutional networks for action segmentation and detection," in *proceedings of the IEEE Conference on Computer Vision and Pattern Recognition*, 2017, pp. 156–165. 1, 3, 8, 13
- [7] Q. Shi, L. Cheng, L. Wang, and A. Smola, "Human action segmentation and recognition using discriminative semi-markov models," *International journal of computer vision*, vol. 93, pp. 22–32, 2011. 1
- [8] S.-J. Li, Y. AbuFarha, Y. Liu, M.-M. Cheng, and J. Gall, "Ms-tcn++: Multi-stage temporal convolutional network for action segmentation," *IEEE transactions on pattern analysis and machine intelligence*, 2020. 1
- [9] T. Lin, X. Liu, X. Li, E. Ding, and S. Wen, "Bmn: Boundary-matching network for temporal action proposal generation," in *Proceedings of the IEEE/CVF international conference on computer vision*, 2019, pp. 3889–3898. 1
- [10] Y.-G. Jiang, J. Liu, A. Roshan Zamir, G. Toderici, I. Laptev, M. Shah, and R. Sukthankar, "THUMOS challenge: Action recognition with a large number of classes," <http://csrcv.ucf.edu/THUMOS14/>, 2014. 1
- [11] S. Vishwakarma and A. Agrawal, "A survey on activity recognition and behavior understanding in video surveillance," *The Visual Computer*, vol. 29, pp. 983–1009, 2013. 1
- [12] E. Apostolidis, E. Adamantidou, A. I. Metsai, V. Mezaris, and I. Patras, "Video summarization using deep neural networks: A survey," *Proceedings of the IEEE*, vol. 109, no. 11, pp. 1838–1863, 2021. 1
- [13] A. Rasouli and J. K. Tsotsos, "Autonomous vehicles that interact with pedestrians: A survey of theory and practice," *IEEE transactions on intelligent transportation systems*, vol. 21, no. 3, pp. 900–918, 2019. 1
- [14] J. Zhang, P.-H. Tsai, and M.-H. Tsai, "Semantic2graph: graph-based multi-modal feature fusion for action segmentation in videos," *Applied Intelligence*, pp. 1–16, 2024. 1, 2, 5
- [15] Y. A. Farha and J. Gall, "Ms-tcn: Multi-stage temporal convolutional network for action segmentation," in *Proceedings of the IEEE/CVF Conference on Computer Vision and Pattern Recognition*, 2019, pp. 3575–3584. 1, 3, 12, 13
- [16] F. Yi, H. Wen, and T. Jiang, "Asformer: Transformer for action segmentation," *arXiv preprint arXiv:2110.08568*, 2021. 1, 3, 12, 13
- [17] Y. Huang, Y. Sugano, and Y. Sato, "Improving action segmentation via graph-based temporal reasoning," in *Proceedings of the IEEE/CVF conference on computer vision and pattern recognition*, 2020, pp. 14 024–14 034. 1, 3
- [18] J. Li, P. Lei, and S. Todorovic, "Weakly supervised energy-based learning for action segmentation," in *Proceedings of the IEEE/CVF International Conference on Computer Vision*, 2019, pp. 6243–6251. 1, 3
- [19] Z. Lu and E. Elhamifar, "Weakly-supervised action segmentation and alignment via transcript-aware union-of-subspaces learning," in *Proceedings of the IEEE/CVF International Conference on Computer Vision*, 2021, pp. 8085–8095. 1, 3
- [20] Y. Souri, M. Fayyaz, L. Minciullo, G. Francesca, and J. Gall, "Fast weakly supervised action segmentation using mutual consistency," *IEEE Transactions on Pattern Analysis and Machine Intelligence*, 2021. 1, 3
- [21] A. Richard, H. Kuehne, and J. Gall, "Action sets: Weakly supervised action segmentation without ordering constraints," in *Proceedings of the IEEE conference on Computer Vision and Pattern Recognition*, 2018, pp. 5987–5996. 1, 3
- [22] J. Li and S. Todorovic, "Set-constrained viterbi for set-supervised action segmentation," in *Proceedings of the IEEE/CVF Conference on Computer Vision and Pattern Recognition*, 2020, pp. 10 820–10 829. 1, 3
- [23] M. Fayyaz and J. Gall, "Sct: Set constrained temporal transformer for set supervised action segmentation," in *Proceedings of the IEEE/CVF Conference on Computer Vision and Pattern Recognition*, 2020, pp. 501–510. 1, 3

- [24] Z. Li, Y. Abu Farha, and J. Gall, “Temporal action segmentation from timestamp supervision,” in *Proceedings of the IEEE/CVF Conference on Computer Vision and Pattern Recognition*, 2021, pp. 8365–8374. 1, 3, 12
- [25] D. Singhania, R. Rahaman, and A. Yao, “Iterative contrast-classify for semi-supervised temporal action segmentation,” in *Proceedings of the AAAI Conference on Artificial Intelligence*, vol. 36, 2022, pp. 2262–2270. 1, 2, 4, 5, 6, 7, 8, 10, 11, 12, 13
- [26] G. Ding and A. Yao, “Leveraging action affinity and continuity for semi-supervised temporal action segmentation,” in *European Conference on Computer Vision*. Springer, 2022, pp. 17–32. 1, 2, 4, 12
- [27] D. Singhania, R. Rahaman, and A. Yao, “C2f-tcn: A framework for semi- and fully-supervised temporal action segmentation,” *IEEE Transactions on Pattern Analysis and Machine Intelligence*, 2023. 1, 13, 14
- [28] T. Chen, S. Kornblith, M. Norouzi, and G. Hinton, “A simple framework for contrastive learning of visual representations,” in *International conference on machine learning*. PMLR, 2020, pp. 1597–1607. 2, 3, 4
- [29] M. Dorkenwald, F. Xiao, B. Brattoli, J. Tighe, and D. Modolo, “Scvrl: Shuffled contrastive video representation learning,” in *Proceedings of the IEEE/CVF Conference on Computer Vision and Pattern Recognition*, 2022, pp. 4132–4141. 2, 3, 6, 1
- [30] Y. Zhu, H. Shuai, G. Liu, and Q. Liu, “Self-supervised video representation learning using improved instance-wise contrastive learning and deep clustering,” *IEEE Transactions on Circuits and Systems for Video Technology*, vol. 32, no. 10, pp. 6741–6752, 2022. 2, 3
- [31] A. Radford, J. W. Kim, C. Hallacy, A. Ramesh, G. Goh, S. Agarwal, G. Sastry, A. Askell, P. Mishkin, J. Clark *et al.*, “Learning transferable visual models from natural language supervision,” in *International conference on machine learning*. PMLR, 2021, pp. 8748–8763. 2
- [32] Y. Ishikawa, S. Kasai, Y. Aoki, and H. Kataoka, “Alleviating over-segmentation errors by detecting action boundaries,” in *Proceedings of the IEEE/CVF winter conference on applications of computer vision*, 2021, pp. 2322–2331. 2
- [33] D. Singhania, R. Rahaman, and A. Yao, “Coarse to fine multi-resolution temporal convolutional network,” *arXiv preprint arXiv:2105.10859*, 2021. 3, 4, 5, 12
- [34] H. Kuehne, J. Gall, and T. Serre, “An end-to-end generative framework for video segmentation and recognition,” in *2016 IEEE Winter Conference on Applications of Computer Vision (WACV)*. IEEE, 2016, pp. 1–8. 3
- [35] B. Singh, T. K. Marks, M. Jones, O. Tuzel, and M. Shao, “A multi-stream bi-directional recurrent neural network for fine-grained action detection,” in *Proceedings of the IEEE conference on computer vision and pattern recognition*, 2016, pp. 1961–1970. 3
- [36] D. Wang, D. Hu, X. Li, and D. Dou, “Temporal relational modeling with self-supervision for action segmentation,” in *Proceedings of the AAAI Conference on Artificial Intelligence*, vol. 35, 2021, pp. 2729–2737. 3
- [37] A. Kukleva, H. Kuehne, F. Sener, and J. Gall, “Unsupervised learning of action classes with continuous temporal embedding,” in *Proceedings of the IEEE/CVF Conference on Computer Vision and Pattern Recognition*, 2019, pp. 12 066–12 074. 3
- [38] S. Sarfraz, N. Murray, V. Sharma, A. Diba, L. Van Gool, and R. Stiefelhagen, “Temporally-weighted hierarchical clustering for unsupervised action segmentation,” in *Proceedings of the IEEE/CVF Conference on Computer Vision and Pattern Recognition*, 2021, pp. 11 225–11 234. 3
- [39] S. Kumar, S. Hareesh, A. Ahmed, A. Konin, M. Z. Zia, and Q.-H. Tran, “Unsupervised action segmentation by joint representation learning and online clustering,” in *Proceedings of the IEEE/CVF Conference on Computer Vision and Pattern Recognition*, 2022, pp. 20 174–20 185. 3
- [40] G. Ding and A. Yao, “Temporal action segmentation with high-level complex activity labels,” *IEEE Transactions on Multimedia*, 2022. 3
- [41] Y. Shi, Z. Wei, H. Ling, Z. Wang, P. Zhu, J. Shen, and P. Li, “Adaptive and robust partition learning for person retrieval with policy gradient,” *IEEE Transactions on Multimedia*, vol. 23, pp. 3264–3277, 2020. 3
- [42] Y. Shi, Z. Wei, H. Ling, Z. Wang, J. Shen, and P. Li, “Person retrieval in surveillance videos via deep attribute mining and reasoning,” *IEEE Transactions on Multimedia*, vol. 23, pp. 4376–4387, 2020. 3
- [43] J. Shen, D. Tao, and X. Li, “Modality mixture projections for semantic video event detection,” *IEEE Transactions on Circuits and Systems for Video Technology*, vol. 18, no. 11, pp. 1587–1596, 2008. 3
- [44] K. He, H. Fan, Y. Wu, S. Xie, and R. Girshick, “Momentum contrast for unsupervised visual representation learning,” in *Proceedings of the IEEE/CVF conference on computer vision and pattern recognition*, 2020, pp. 9729–9738. 3, 4
- [45] A. v. d. Oord, Y. Li, and O. Vinyals, “Representation learning with contrastive predictive coding,” *arXiv preprint arXiv:1807.03748*, 2018. 3, 4
- [46] Y. Tian, D. Krishnan, and P. Isola, “Contrastive multiview coding,” in *European conference on computer vision*. Springer, 2020, pp. 776–794. 3
- [47] K. Hu, J. Shao, Y. Liu, B. Raj, M. Savvides, and Z. Shen, “Contrast and order representations for video self-supervised learning,” in *Proceedings of the IEEE/CVF International Conference on Computer Vision*, 2021, pp. 7939–7949. 3
- [48] R. Qian, T. Meng, B. Gong, M.-H. Yang, H. Wang, S. Belongie, and Y. Cui, “Spatiotemporal contrastive video representation learning,” in *Proceedings of the IEEE/CVF Conference on Computer Vision and Pattern Recognition*, 2021, pp. 6964–6974. 3
- [49] A. Recasens, P. Luc, J.-B. Alayrac, L. Wang, F. Strub, C. Tallec, M. Malinowski, V. Pătrăucean, F. Altché, M. Valko *et al.*, “Broaden your views for self-supervised video learning,” in *Proceedings of the IEEE/CVF International Conference on Computer Vision*, 2021, pp. 1255–1265. 3
- [50] S. Biswas and J. Gall, “Multiple instance triplet loss for weakly supervised multi-label action localisation of interacting persons,” in *Proceedings of the IEEE/CVF International Conference on Computer Vision*, 2021, pp. 2159–2167. 3, 6
- [51] E. Eldele, M. Ragab, Z. Chen, M. Wu, C. K. Kwok, X. Li, and C. Guan, “Time-series representation learning via temporal and contextual contrasting,” *arXiv preprint arXiv:2106.14112*, 2021. 3
- [52] Z. Yue, Y. Wang, J. Duan, T. Yang, C. Huang, Y. Tong, and B. Xu, “Ts2vec: Towards universal representation of time series,” in *Proceedings of the AAAI Conference on Artificial Intelligence*, vol. 36, 2022, pp. 8980–8987. 3
- [53] J.-Y. Franceschi, A. Dieuleveut, and M. Jaggi, “Unsupervised scalable representation learning for multivariate time series,” *Advances in neural information processing systems*, vol. 32, 2019. 3, 5, 6
- [54] F. Schroff, D. Kalenichenko, and J. Philbin, “Facenet: A unified embedding for face recognition and clustering,” in *Proceedings of the IEEE conference on computer vision and pattern recognition*, 2015, pp. 815–823. 3, 5
- [55] W. Ge, “Deep metric learning with hierarchical triplet loss,” in *Proceedings of the European Conference on Computer Vision (ECCV)*, 2018, pp. 269–285. 3
- [56] F. Boutros, N. Damer, F. Kirchbuchner, and A. Kuijper, “Self-restrained triplet loss for accurate masked face recognition,” *Pattern Recognition*, vol. 124, p. 108473, 2022. 3, 6
- [57] J. Zhang, L. Gao, X. Luo, H. Shen, and J. Song, “Data: Denoised task adaptation for few-shot learning,” in *Proceedings of the IEEE/CVF International Conference on Computer Vision*, 2023, pp. 11 541–11 551. 3
- [58] M. Afham and R. Rodrigo, “Visual-semantic contrastive alignment for few-shot image classification,” *arXiv preprint arXiv:2210.11000*, 2022. 3
- [59] J. Zhang, J. Song, L. Gao, Y. Liu, and H. T. Shen, “Progressive meta-learning with curriculum,” *IEEE Transactions on Circuits and Systems for Video Technology*, vol. 32, no. 9, pp. 5916–5930, 2022. 3
- [60] J. Zhang, L. Gao, B. Hao, H. Huang, J. Song, and H. Shen, “From global to local: Multi-scale out-of-distribution detection,” *IEEE Transactions on Image Processing*, 2023. 3
- [61] S. Mo, J.-C. Su, C.-Y. Ma, M. Assran, I. Misra, L. Yu, and S. Bell, “Ropaws: Robust semi-supervised representation learning from uncurated data,” *arXiv preprint arXiv:2302.14483*, 2023. 3
- [62] D.-H. Lee *et al.*, “Pseudo-label: The simple and efficient semi-supervised learning method for deep neural networks,” in *Workshop on challenges in representation learning, ICML*, vol. 3, no. 2. Atlanta, 2013, p. 896. 3
- [63] Q. Xie, M.-T. Luong, E. Hovy, and Q. V. Le, “Self-training with noisy student improves imagenet classification,” in *Proceedings of the IEEE/CVF conference on computer vision and pattern recognition*, 2020, pp. 10 687–10 698. 3
- [64] M. N. Rizve, K. Duarte, Y. S. Rawat, and M. Shah, “In defense of pseudo-labeling: An uncertainty-aware pseudo-label selection framework for semi-supervised learning,” *arXiv preprint arXiv:2101.06329*, 2021. 3
- [65] K. Sohn, D. Berthelot, N. Carlini, Z. Zhang, H. Zhang, C. A. Raffel, E. D. Cubuk, A. Kurakin, and C.-L. Li, “Fixmatch: Simplifying semi-supervised learning with consistency and confidence,” *Advances in neural information processing systems*, vol. 33, pp. 596–608, 2020. 3, 12

- [66] T. Miyato, S.-i. Maeda, M. Koyama, and S. Ishii, "Virtual adversarial training: a regularization method for supervised and semi-supervised learning," *IEEE transactions on pattern analysis and machine intelligence*, vol. 41, no. 8, pp. 1979–1993, 2018. 3
- [67] Y. Tang, W. Chen, Y. Luo, and Y. Zhang, "Humble teachers teach better students for semi-supervised object detection," in *Proceedings of the IEEE/CVF Conference on Computer Vision and Pattern Recognition*, 2021, pp. 3132–3141. 3
- [68] J. Wu, W. Sun, T. Gan, N. Ding, F. Jiang, J. Shen, and L. Nie, "Neighbor-guided consistent and contrastive learning for semi-supervised action recognition," *IEEE Transactions on Image Processing*, 2023. 3
- [69] T. Chen, S. Kornblith, K. Swersky, M. Norouzi, and G. E. Hinton, "Big self-supervised models are strong semi-supervised learners," *Advances in neural information processing systems*, vol. 33, pp. 22 243–22 255, 2020. 4
- [70] Z. Cai, A. Ravichandran, P. Favaro, M. Wang, D. Modolo, R. Bhotika, Z. Tu, and S. Soatto, "Semi-supervised vision transformers at scale," *Advances in Neural Information Processing Systems*, vol. 35, pp. 25 697–25 710, 2022. 4
- [71] M. Assran, M. Caron, I. Misra, P. Bojanowski, A. Joulin, N. Ballas, and M. Rabbat, "Semi-supervised learning of visual features by non-parametrically predicting view assignments with support samples," in *Proceedings of the IEEE/CVF International Conference on Computer Vision*, 2021, pp. 8443–8452. 4
- [72] J. Carreira and A. Zisserman, "Quo vadis, action recognition? a new model and the kinetics dataset," in *proceedings of the IEEE Conference on Computer Vision and Pattern Recognition*, 2017, pp. 6299–6308. 5
- [73] Z. Ming, J. Chazalon, M. M. Luqman, M. Visani, and J.-C. Burie, "Simple triplet loss based on intra/inter-class metric learning for face verification," in *2017 IEEE International Conference on Computer Vision Workshops (ICCVW)*. IEEE, 2017, pp. 1656–1664. 6
- [74] P. Zhang, C. Lan, W. Zeng, J. Xing, J. Xue, and N. Zheng, "Semantics-guided neural networks for efficient skeleton-based human action recognition," in *proceedings of the IEEE/CVF conference on computer vision and pattern recognition*, 2020, pp. 1112–1121. 8
- [75] F. Sener, D. Singhania, and A. Yao, "Temporal aggregate representations for long-range video understanding," in *European Conference on Computer Vision*. Springer, 2020, pp. 154–171. 8
- [76] S. Stein and S. J. McKenna, "Combining embedded accelerometers with computer vision for recognizing food preparation activities," in *Proceedings of the 2013 ACM international joint conference on Pervasive and ubiquitous computing*, 2013, pp. 729–738. 8
- [77] A. Fathi, X. Ren, and J. M. Rehg, "Learning to recognize objects in egocentric activities," in *CVPR 2011*. IEEE, 2011, pp. 3281–3288. 8
- [78] H. Kuehne, A. Arslan, and T. Serre, "The language of actions: Recovering the syntax and semantics of goal-directed human activities," in *Proceedings of the IEEE conference on computer vision and pattern recognition*, 2014, pp. 780–787. 8
- [79] F. Zhou, Z. Jiang, Z. Liu, F. Chen, L. Chen, L. Tong, Z. Yang, H. Wang, M. Fei, L. Li *et al.*, "Structured context enhancement network for mouse pose estimation," *IEEE Transactions on Circuits and Systems for Video Technology*, vol. 32, no. 5, pp. 2787–2801, 2021. 8, 3
- [80] Z. Jiang, F. Zhou, A. Zhao, X. Li, L. Li, D. Tao, X. Li, and H. Zhou, "Multi-view mouse social behaviour recognition with deep graph model," *IEEE Transactions on Image Processing*, vol. 30, pp. 5490–5504, 2021. 8, 13, 2
- [81] Z. Jiang, Z. Liu, L. Chen, L. Tong, X. Zhang, X. Lan, D. Crookes, M.-H. Yang, and H. Zhou, "Detecting and tracking of multiple mice using part proposal networks," *IEEE Transactions on Neural Networks and Learning Systems*, vol. 34, no. 12, pp. 9806–9820, 2023. 8
- [82] F. Zhou, X. Yang, F. Chen, L. Chen, Z. Jiang, H. Zhu, R. Heckel, H. Wang, M. Fei, and H. Zhou, "Cross-skeleton interaction graph aggregation network for representation learning of mouse social behaviour," *arXiv preprint arXiv:2208.03819*, 2022. 8, 13, 3
- [83] M.-H. Chen, B. Li, Y. Bao, G. AlRegib, and Z. Kira, "Action segmentation with joint self-supervised temporal domain adaptation," in *Proceedings of the IEEE/CVF Conference on Computer Vision and Pattern Recognition*, 2020, pp. 9454–9463. 12
- [84] J. Wang, Z. Wang, S. Zhuang, and H. Wang, "Cross-enhancement transformer for action segmentation," *arXiv preprint arXiv:2205.09445*, 2022. 12
- [85] D. Liu, Q. Li, A. Dinh, T. Jiang, M. Shah, and C. Xu, "Diffusion action segmentation," in *Proceedings of the IEEE/CVF International Conference on Computer Vision*, 2023. 12
- [86] L. Yang, L. Qi, L. Feng, W. Zhang, and Y. Shi, "Revisiting weak-to-strong consistency in semi-supervised semantic segmentation," in *Proceedings of the IEEE/CVF Conference on Computer Vision and Pattern Recognition*, 2023, pp. 7236–7246. 12, 13
- [87] A. Tarvainen and H. Valpola, "Mean teachers are better role models: Weight-averaged consistency targets improve semi-supervised deep learning results," *Advances in neural information processing systems*, vol. 30, 2017. 12
- [88] Z. Jiang, D. Crookes, B. D. Green, Y. Zhao, H. Ma, L. Li, S. Zhang, D. Tao, and H. Zhou, "Context-aware mouse behavior recognition using hidden markov models," *IEEE Transactions on Image Processing*, vol. 28, no. 3, pp. 1133–1148, 2018. 2
- [89] T. D. Pereira, J. W. Shaveitz, and M. Murthy, "Quantifying behavior to understand the brain," *Nature neuroscience*, vol. 23, no. 12, pp. 1537–1549, 2020. 2
- [90] V. Jackson-Lewis and S. Przedborski, "Protocol for the mptp mouse model of parkinson's disease," *Nature protocols*, vol. 2, no. 1, p. 141, 2007. 2

SUPPLEMENTARY A

Additional qualitative results. As shown in Fig. S1, we visualise the I3D feature and other features learned by ICC and our method using t-Distributed Stochastic Neighbor Embedding (t-SNE) on GTEA datasets. Different colours represent different actions. Our approach leads to better separation of different classes, demonstrating the strong representation learning ability of our Semantic-guided Multi-level Contrast scheme.

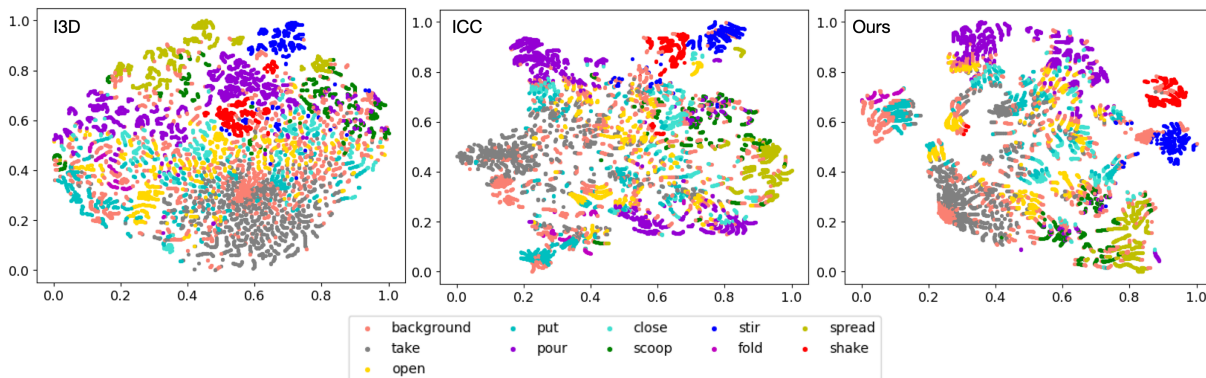


Fig. S1. t-SNE visualisation of the I3D feature and other features learned by ICC and our method. Each point represents an image frame. We show all behaviour classes (11) of the GTEA dataset in different colours.

Compare SMC with other unsupervised representation learning methods. In Tab. 3 (main paper) of the paper, we have compared our unsupervised method with that of ICC. Since ICC is the first work based on unsupervised representation learning for semi-supervised action segmentation, so far we could not find any other publications exploring unsupervised representation learning for this task. Thus, we attempt to compare our unsupervised method against a SOTA method [29] of unsupervised video representation learning, but it is not quite related to this task. We use the same positive and anchor representations as those of our work but the negative representation is obtained by temporal shuffling [29] of anchor representation. From Tab. S1, our method shows better performance.

TABLE S1
COMPARING OUR SMC WITH SCVRL [29].

Dataset	Method	F1@{10, 25, 50}			Edit	Acc
50Salads	SCVRL [29]	48.0	43.5	34.4	37.8	69.2
	SMC	58.1	54.0	43.5	46.3	75.1
GTEA	SCVRL [29]	72.5	66.0	48.6	64.9	71.2
	SMC	78.9	74.3	59.2	73.0	76.2
Breakfast	SCVRL [29]	46.8	41.9	31.8	38.6	71.1
	SMC	59.7	55.4	42.8	52.7	72.1

TABLE S2
TRAINING HYPERPARAMETERS LEARNING RATE (LR), WEIGHT-DECAY (WD), EPOCHS (Eps.) AND BATCH SIZE (BS) OVER DIFFERENT DATASETS FOR UNSUPERVISED AND SEMI-SUPERVISED LEARNING.

Model	Breakfast				50Salads				GTEA				PDMB			
	LR	WD	Eps.	BS	LR	WD	Eps.	BS	LR	WD	Eps.	BS	LR	WD	Eps.	BS
(T: S)	1e-3	3e-3	100	50	1e-3	1e-3	100	5	1e-3	3e-4	100	4	1e-3	3e-4	100	4
C	1e-2	3e-3	200	50	1e-2	1e-3	400	5	1e-2	3e-4	400	4	1e-2	3e-4	400	4
(T:G:S)	1e-5	3e-3	200	50	1e-5	1e-3	400	5	1e-5	3e-4	400	4	1e-5	3e-4	400	4

SUPPLEMENTARY B

TABLE S3
ETHOGRAM OF THE OBSERVED BEHAVIOURS [80].

Behaviour	Description
approach	Moving toward another mouse in a straight line without obvious exploration.
chase	A following mouse attempts to maintain a close distance to another mouse while the latter is moving.
circle	Circling around own axis or chasing tail.
eat	Gnawing/eating food pellets held by the fore-paws.
clean	Washing the muzzle with fore-paws (including licking fore-paws) or grooming the fur or hind-paws by means of licking or chewing.
sniff	Sniff any body part of another mouse.
up	Exploring while standing in an upright posture.
walk away	Moving away from another mouse in a straight line without obvious exploration.
other	behaviour other than defined in this ethogram, or when it is not visible what behaviour the mouse displays.

Additional related works about temporal modelling of mouse behaviour. In recent years, temporal dependencies among actions have also been investigated to facilitate mouse behaviour modelling. Jiang et al. [88] employed a Hidden Markov Model (HMM) to model the contextual relationship among adjacent mouse behaviours over time. Specifically, they represented each action clip as a set of feature vectors using spatial-temporal Segment Fisher Vectors (SFV), which were then treated as observed variables in the HMM. In addition, Jiang et al. [80] proposed a deep graphic model to explore the temporal correlations of mouse social behaviours, which demonstrated the advantage of modelling behavioural correlations. However, these methods mainly focus on the correlations between the neighbouring behaviours, which is difficult to capture multi-scale temporal dependencies of mouse behaviours in long videos. Also, these methods usually require fully supervised data, which is obtained by manually annotating the exact temporal location of each behaviour occurring in all training videos. Such data collection is expensive, particularly in behavioural neuroscience [89], where datasets are usually complex and lab-specific.

TABLE S4

COMPONENT-WISE ANALYSIS OF THE UNSUPERVISED REPRESENTATION LEARNING FRAMEWORK WITH A LINEAR CLASSIFIER ON THE PDMB DATASET.

Method	PDMB				
	F1@{10, 25, 50}			Edit	Acc
$\mathcal{L}_{ap}^P(\mathbf{M}_{in}) + \mathcal{L}_{aa}^N$	39.0	33.9	21.6	36.5	37.7
$\mathcal{L}_{ap}^P(\mathbf{I}) + \mathcal{L}_{aa}^N$	56.3	53.6	40.8	51.8	53.4
$\mathcal{L}_{ap}^P(\mathbf{M}_{in}) + \mathcal{L}_{ap}^N$	38.0	34.2	24.3	35.3	42.2
$\mathcal{L}_{ap}^P(\mathbf{I}) + \mathcal{L}_{ap}^N$	55.9	53.5	41.0	40.1	54.3
<i>Constructing positive pairs by \mathbf{M}_{in} or \mathbf{I}</i>					
$\mathcal{L}_{ap}^P + \mathcal{L}_{aa}^N$	56.3	53.6	40.8	51.8	53.4
$\mathcal{L}_{ap}^P + \mathcal{L}_{ap}^N$	55.9	53.5	41.0	40.1	54.3
$\mathcal{L}_{ap}^P + \mathcal{L}_{aa}^N + \mathcal{L}_{ap}^N$	58.5	56.6	43.6	53.4	58.5
$\mathcal{L}_{ap}^P + \mathcal{L}_{aa}^N + \mathcal{L}_{ap}^N + \mathcal{L}_{pp}^N$	59.6	58.0	45.9	53.8	61.3
<i>Comparing different negative pairs</i>					
w/o dynamic clustering	59.6	58.0	45.9	53.8	61.3
w/ dynamic clustering	61.1	59.6	47.2	55.5	62.5
<i>Dynamic clustering facilitates contrastive learning</i>					

Mouse Social Behaviour Dataset. Our Parkinson’s Disease Mouse Behaviour (PDMB) dataset was collected in collaboration with the biologists of Queen’s University Belfast of United Kingdom, for a study on motion recordings of mice with Parkinson’s disease (PD) [80]. The neurotoxin 1-methyl-4-phenyl-1,2,3,6-tetrahydropyridine (MPTP) is used as a model of PD, which has become an invaluable aid to produce experimental parkinsonism since its discovery in 1983 [90]. All experimental procedures were performed in accordance with the Guidance on the Operation of the Animals (Scientific Procedures) Act, 1986 (UK) and approved by the Queen’s University Belfast Animal Welfare and Ethical Review Body. We recorded videos for 3 groups of MPTP treated mice and 3 groups of control mice by using three synchronised Sony Action cameras (HDR-AS15) (one top-view and two side-view) with frame rate of 30 fps and 640*480 resolution. Each group consists of 6 annotated videos and

TABLE S5
PERFORMANCE OF THE NCA MODULE ON OUR PDMB DATASET (10%).

Dataset	Method	F1@{10, 25, 50}			Edit	Acc
PDMB	w/o \mathcal{L}_{nca}	54.7	48.7	31.9	45.0	52.7
	w/ \mathcal{L}_{nca}	62.0	57.1	40.7	52.7	55.1
	Gain	7.3	8.4	8.8	7.7	2.4

all videos contain 9 behaviours (defined in Tab. S3) of two freely behaving mice. Different from the experiments of human action segmentation, the input features we use in experiments on this dataset are extracted from the pre-trained model from [82], which encodes the social interactions of mice based on the pose information [79]. The whole dataset is evenly divided into training and testing datasets, and we select 10% or 50% of the videos from the training split for the labelled dataset \mathcal{D}_L .

Evaluation of Representation Learning on the PDMB Dataset. As shown in Tab. S4, on the PDMB dataset, utilising M_{in} would also lead to the generation of pseudo positive pairs, which would impede the efficacy of contrastive learning and consequently result in a significant performance drop. Besides, we achieve the best performance for all metrics when combining three types of negative pairs at the same time, where such combination brings gains of 7.9% and 7% in accuracy for the settings with only \mathcal{L}_{aa}^N and \mathcal{L}_{ap}^N , respectively.

Effect of the NCA Unit on the PDMB Dataset. As shown in Tab. S5, with respect to behavioural correlation modelling of mice, we achieve a significant improvement of more than 7% in F1 and Edit scores on the PDMB dataset.

Finally, to demonstrate the applicability of the proposed framework to behaviour phenotyping of the mice with Parkinson’s disease, we investigate the behavioural correlations of both MPTP treated mice and their control strains, as shown in Fig. S2. The findings reveal that MPTP treated mice are more likely to perform ‘approach’ after ‘circle’, ‘up’ or ‘walk_away’ compared to the control group (‘other’ is excluded). Besides, MPTP treated mice tend to exhibit ‘sniff’ behaviour while the normal mice show a higher propensity towards ‘walk_away’ after ‘chase’.

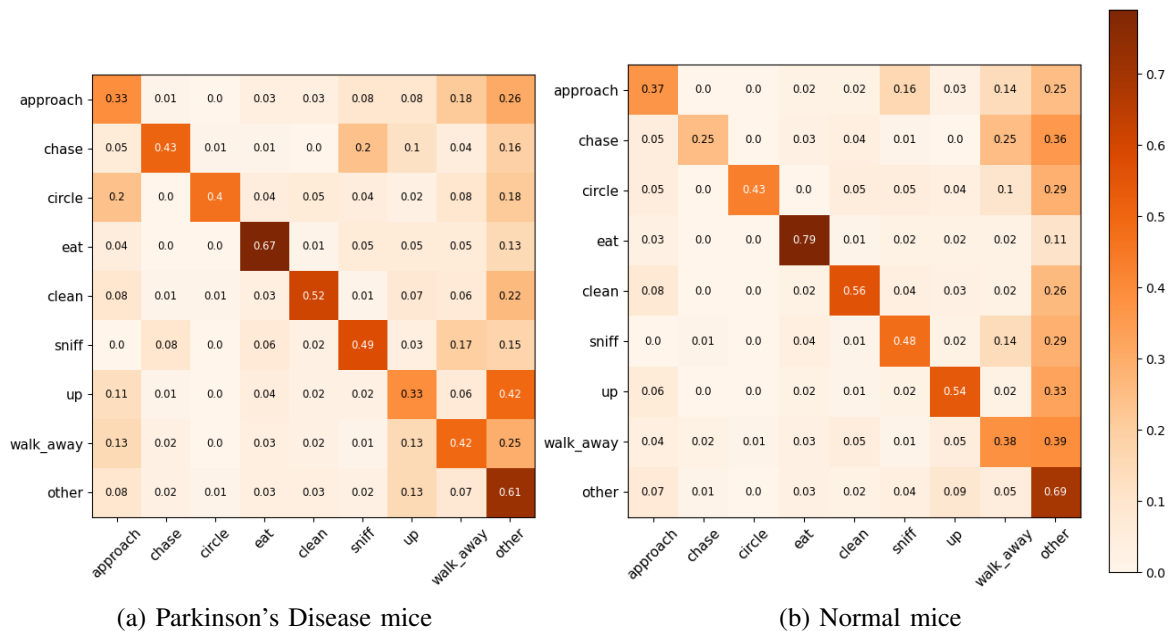


Fig. S2. Occurrence frequency of neighbouring behaviours (20-frame interval) for Parkinson’s Disease and normal mice. Each cell contains the percentage of the occurrence of behaviour x (along rows) after behaviour y (along column) appears.